New materials which might be presented at ALCW 2018

Natural SUSY with light higgsinos

Keisuke Fujii (KEK)

ILD S&A Meeting, May 23, 2018

This talk will update one given by Tomohiko in Strasbourg on October 24, 2017.

Tomohiko showed the updated results in the S&A meeting on December 20, 2018

More complete BG (missing phase space in low ee-pair invariant mass plugged, 2-photon ae→3f included

Consistent selection cuts for all benchmarks, final states, and beam polarizations

Global mass fits with improved edge detection

Suvi's new plots for Model parameter extractions

PMQ	ILC1	ILC2	nGMM1
m_0	7025.0	5000	$m_{3/2} = 75000$
$m_{1/2}$ / M_1, M_2, M_3	568.3	1200	3382.5, 2124.4, 1225.8
A_0	-10427	-8000	$a_3 = 3$
$\tan\beta$	10	15	10
other	–	–	$c_m = 6.9;\ \alpha = 4$
m_h	125.3	125.4	124.9
m_A	1000.0	1000	2000
m_H	1006.8	1006.7	2013.3
$m_{H^\pm}$	1003.2	1003.2	2001.6
μ	115.0	150	150
$m_{\tilde{g}}$	1563.5	2832.6	2856.5
$m_{\tilde{\chi}^\pm_{1,2}}$	117.3, 513.0	158.3, 1017.5	158.7, 1791.6
$m_{\tilde{\chi}^0_{1,2}}$	102.7, 124.0	148.1, 157.8	151.4, 155.8
$m_{\tilde{\chi}^0_{3,4}}$	267.0, 524.2	538.7, 1031.1	1526.9, 1799.4
$m_{\tilde{u}_{L,R}}$	7021.3, 7254.2	5440.4, 5565.6	5266.7, 5398.2
$m_{\tilde{t}_{1,2}}$	1893.3, 4919.4	1774.3, 3877.9	1433.1, 3732.0
$m_{\tilde{d}_{L,R}}$	7021.8, 6998.6	5441.0, 5384.5	5267.3, 5228.6
$m_{\tilde{b}_{1,2}}$	4959.2, 6893.3	3902.8, 5204.5	3770.5, 5124.5
$m_{\tilde{e}_{L,R}}$	7152.5, 6758.6	5149.0, 4817.1	5127.8, 4824.6
$m_{\tilde{\tau}_{1,2}}$	6656.6, 7103.1	4652.3, 5072.5	4749.5, 5093.9
$\Omega^{std}_{\tilde{\chi}^0}h^2$	0.009	0.007	0.005
$\langle\sigma v\rangle(v\to 0)$ [cm^3/s]	2.2×10^{-25}	2.9×10^{-25}	3.1×10^{-25}
$\sigma^{SI}(\tilde{\chi}^0 p)\times 10^9$ [pb]	6.8	1.5	0.3
$a_\mu^{SUSY}\times 10^{10}$	0.03	0.13	0.06
$BF(b\to s\gamma)\times 10^4$	3.3	3.3	3.1
$BF(B_S\to\mu^+\mu^-)\times 10^9$	3.8	3.8	3.8
$BF(B_u\to\tau\nu_\tau)\times 10^4$	1.3	1.3	1.3
Δ_{EW}	14	28	15

Table 1: Input parameters and mass spectrum and rates for benchmark points ILC1, ILC2 and nGMM1. All masses and dimensionful parameters are in GeV units. All values have been obtained with Isasugra. The nGMM1 benchmark has parameters $\alpha = 4$ and $m_{3/2} = 75$ TeV with $c_m = 6.9$ and $a_3 = 3$.

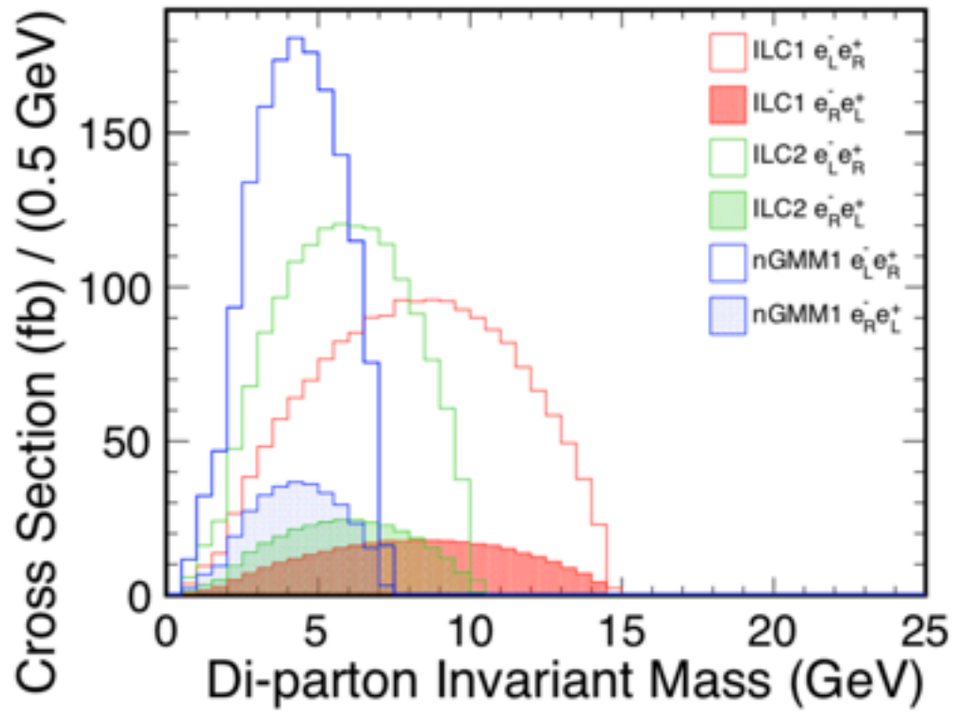

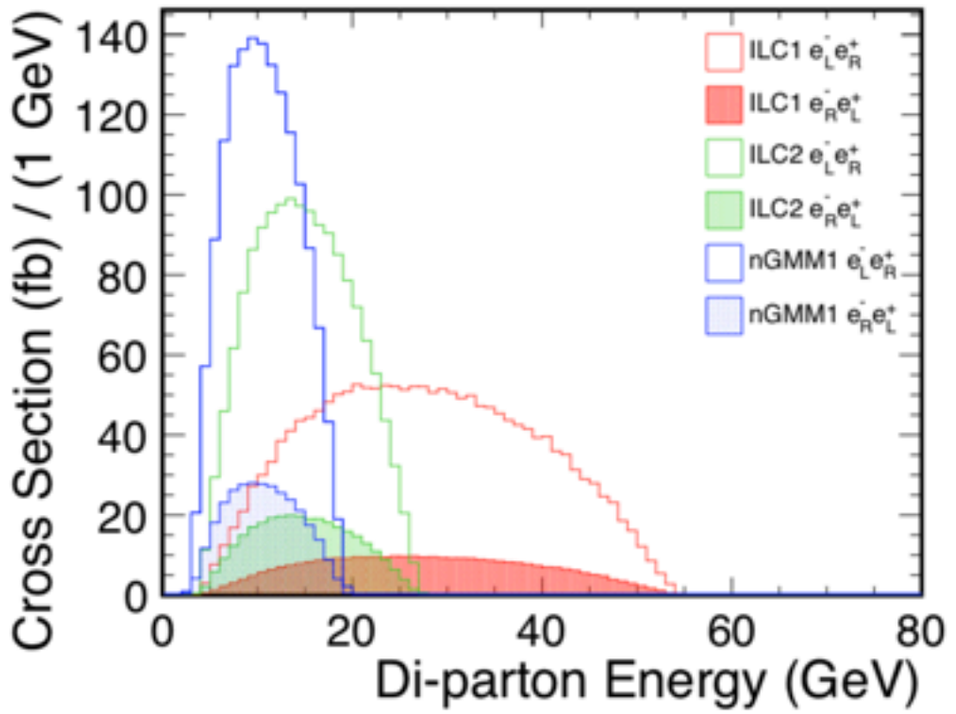

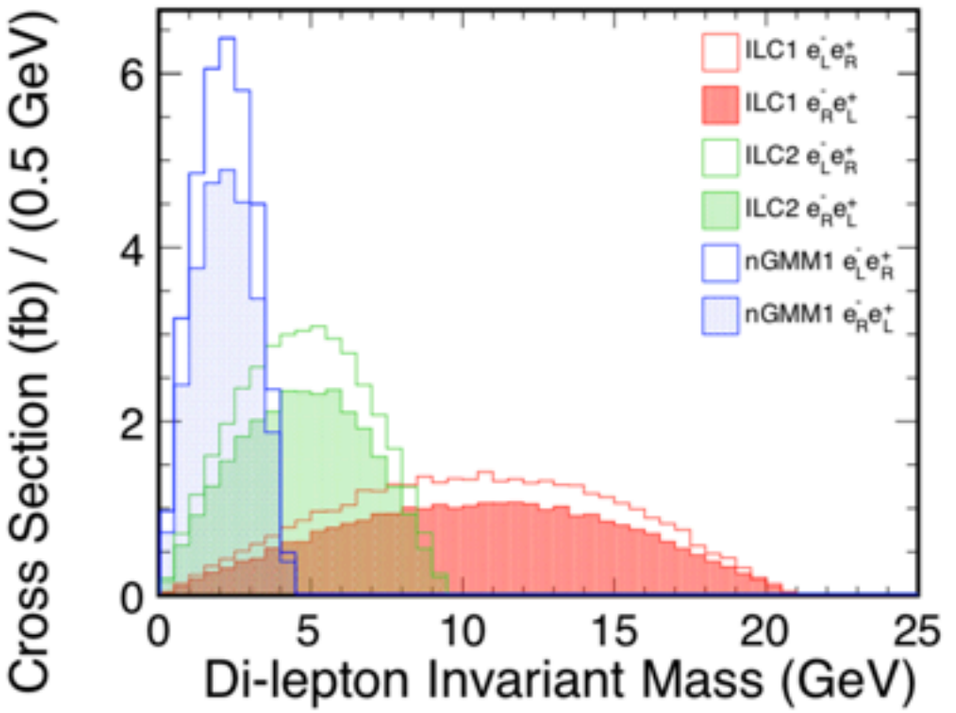

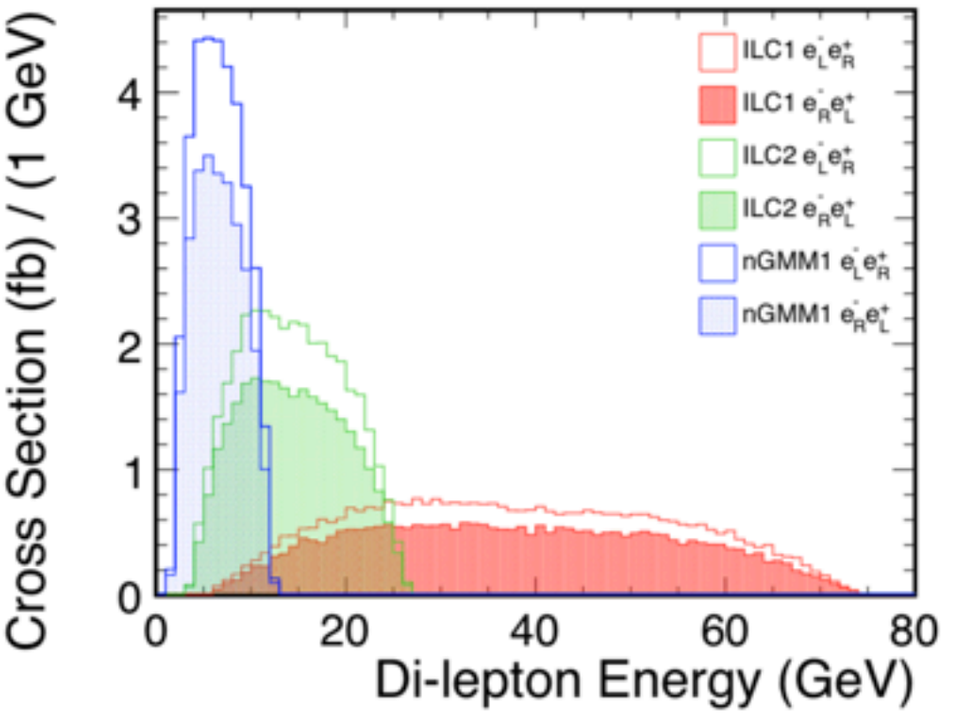

Figure 3: The generator-level distributions of the key observables. The di-jet invariant mass and energy distributions are shown for the chargino channel, while the di-lepton invariant mass and energy distributions are shown for the neutralino channel.

Missing Phase Space

Tomohiko

Previously missing phase space in 4-fermion backgrounds (due to generator-level cut) is now supplemented by including additional samples (full/fast)

[Thanks to H. Ono, A. Miyamoto, M. Berggren]

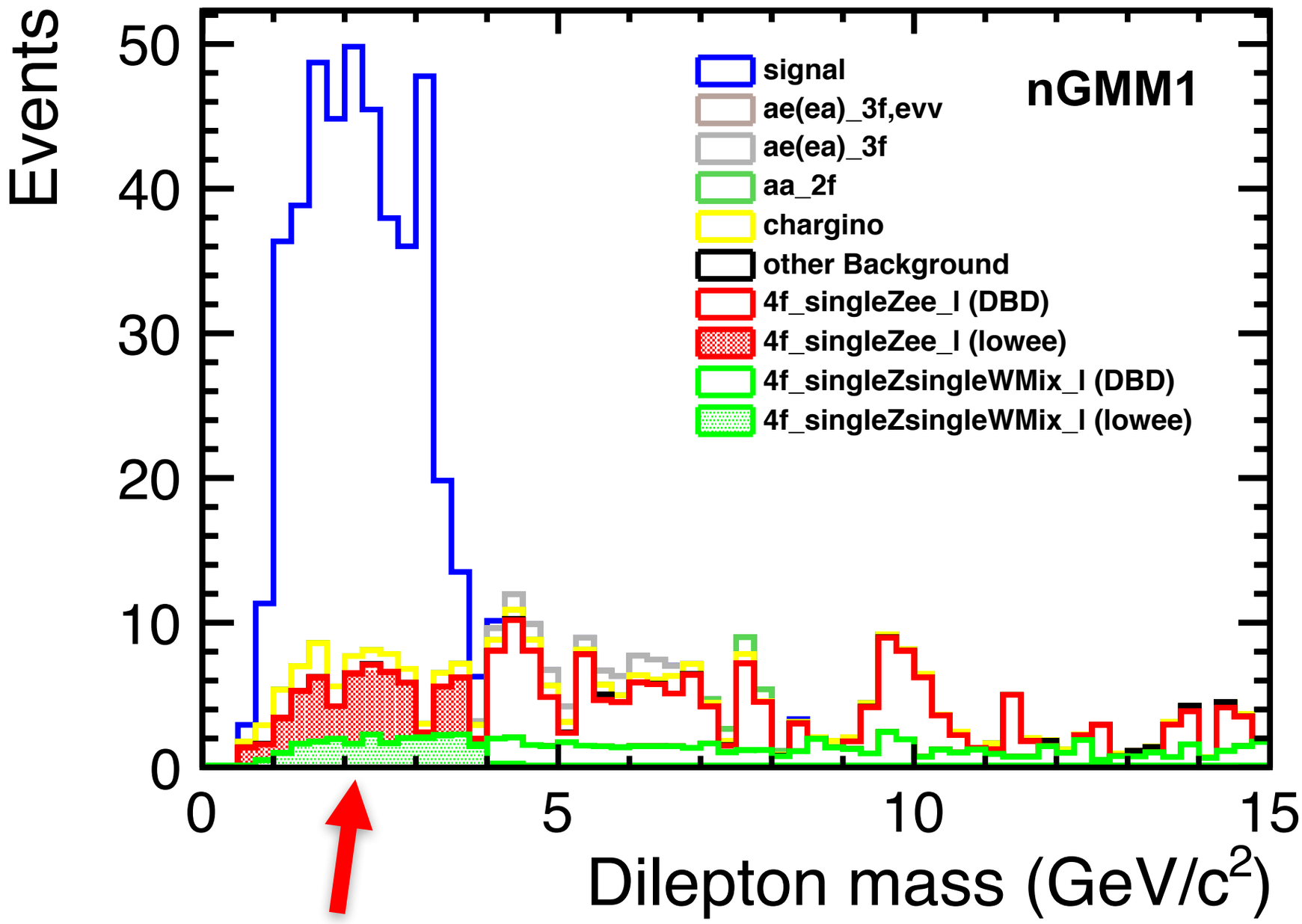

Event Selection (N1N2)

1. Pair of isolated leptons (e or μ) **[preselelection]**
2. Visible Energy in the event < 25 GeV
3. Missing Energy in the event 300 GeV
4. Missing $|\cos\theta| < 0.98$
5. No BeamCal hits
6. # of tracks with pT>2 GeV = 2
7. Lepton pT > 2.3 GeV, $|\cos\theta| < 0.95$
8. di-lepton coplanarity < 0.8
9. di-lepton $|\cos\theta| < 0.98$
10. **di-lepton mass cuts for di-lepton energy measurement (process-dependent)**

Consistent across all benchmarks (ILC1/ILC2/nGMM1) **[except #10]**, final states (e/mu), and beam polarizations.

Event Selection (C1C1)

1. One isolated lepton (e or μ) **[preselelection]**
2. No BeamCal hits
3. **Lepton pT > 5 GeV (suppress two-photon background)**
4. **# of tracks in event >= 4 (suppress ae_3f background)**
5. Missing Energy > 400 GeV
6. Missing $|\cos\theta| < 0.99$
7. Visible Energy < 80 GeV
8. Each jet $|\cos\theta| < 0.98$
9. di-jet coplanarity < 1.0
10. Angle between lepton and dijet system $|\cos\theta| < 0.2$

Consistent across all benchmarks (ILC1/ILC2/nGMM1), final states (e/mu), and beam polarizations.

The event selection is much tighter compared to previous results. This is to ensure the removal of the 2-photon and ae_3f backgrounds.

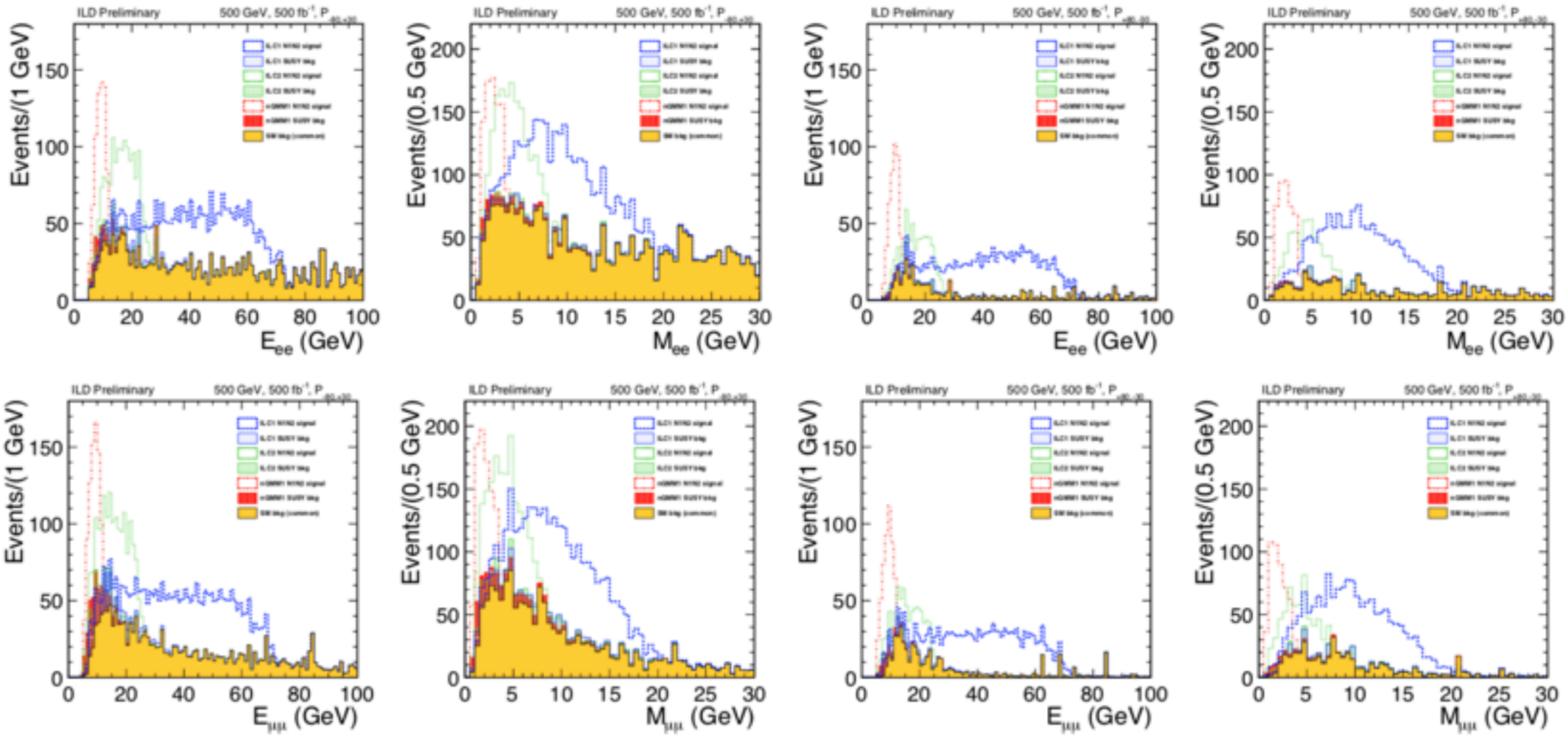

Figure 5: Neutralino measurement

Kinematic Edges: ILC1 (N1N2)

ee, (-80,+30) **ee, (+80,-30)** **μμ, (-80,+30)** **μμ, (+80,-30)**

M

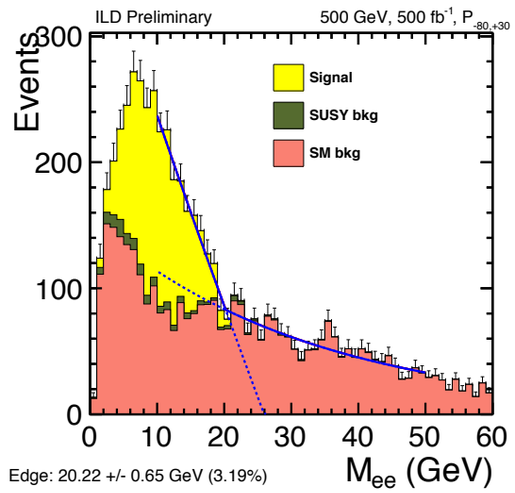

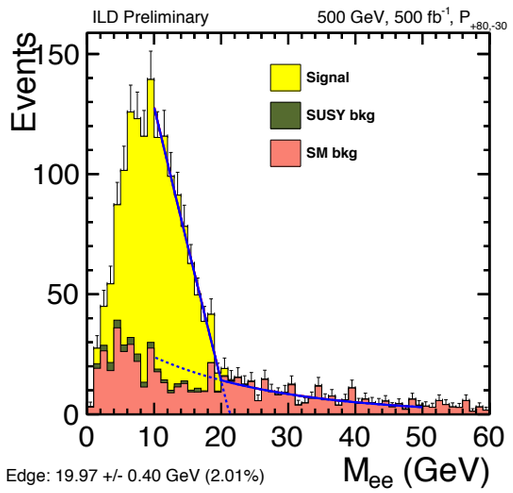

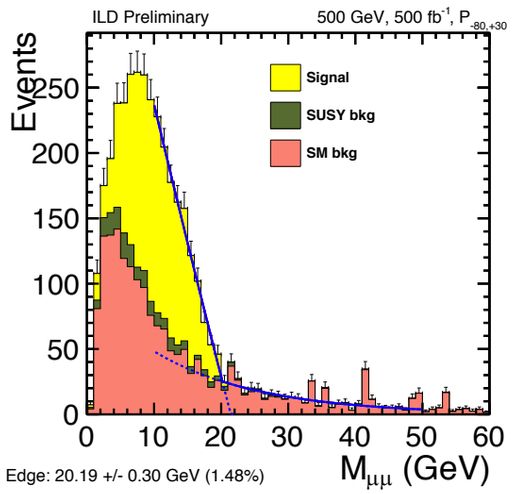

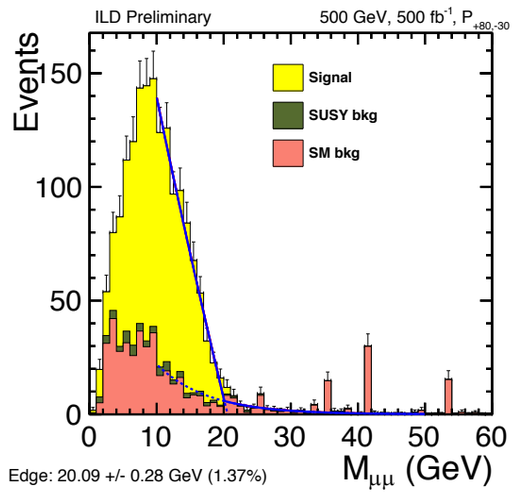

E

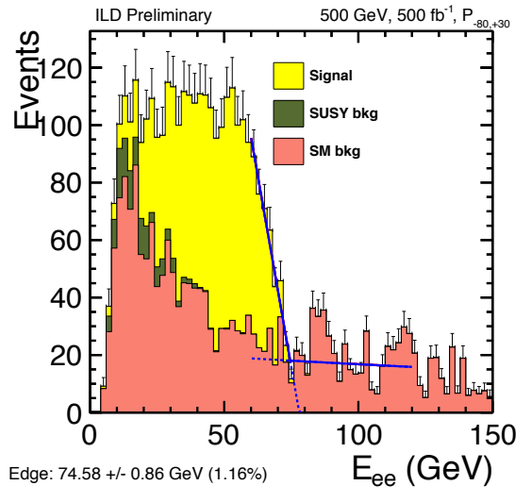

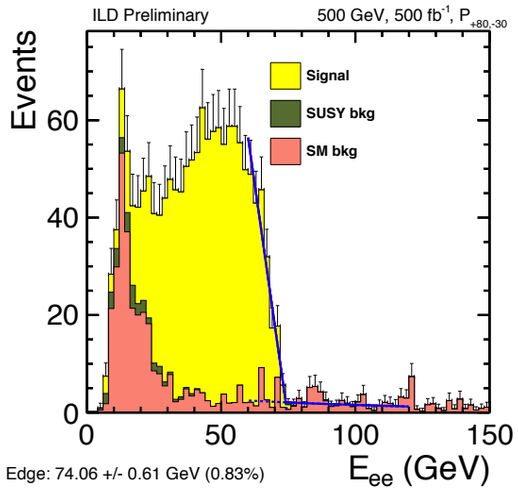

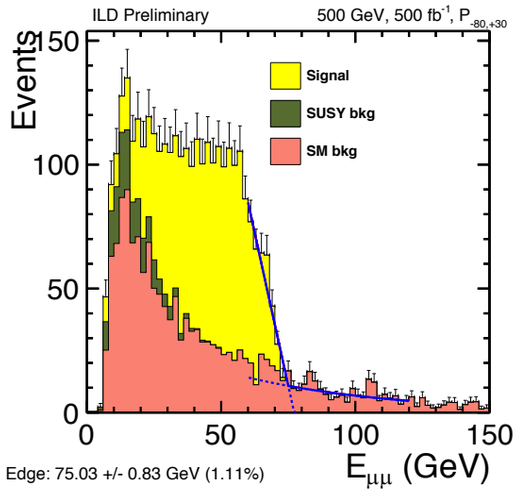

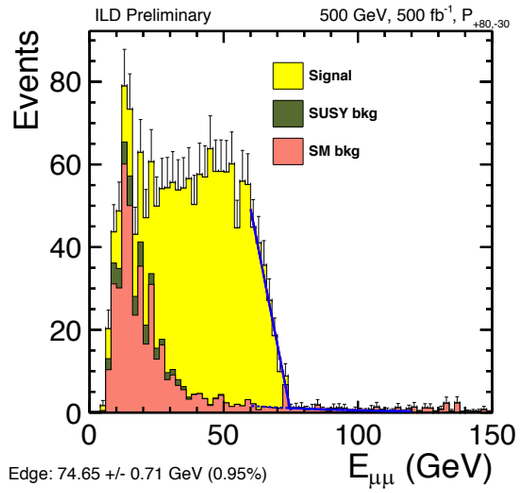

The kinematic edge is modeled as: straight line (signal) + exponential (background). The precision is estimated using toy MC experiments.

Kinematic Edges: ILC2 (N1N2)

	ee, (-80,+30)	ee, (+80,-30)	μμ, (-80,+30)	μμ, (+80,-30)
M	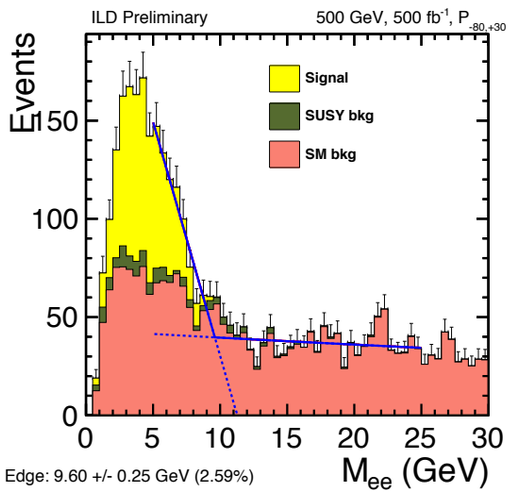 Edge: 9.60 +/- 0.25 GeV (2.59%)	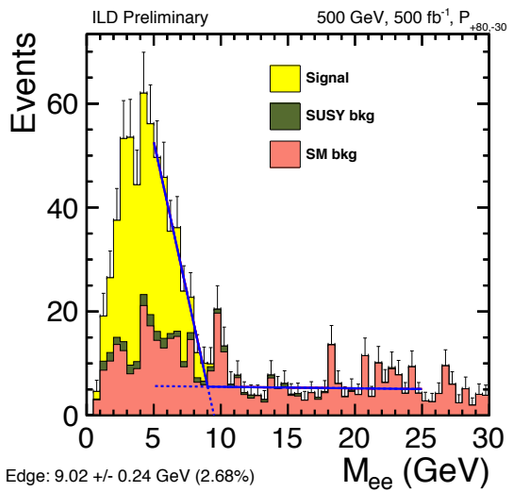 Edge: 9.02 +/- 0.24 GeV (2.68%)	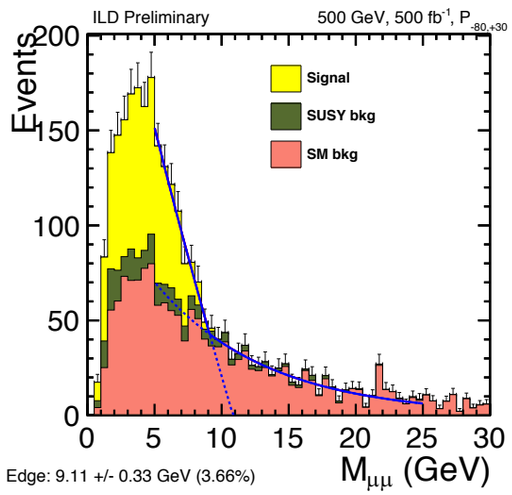 Edge: 9.11 +/- 0.33 GeV (3.66%)	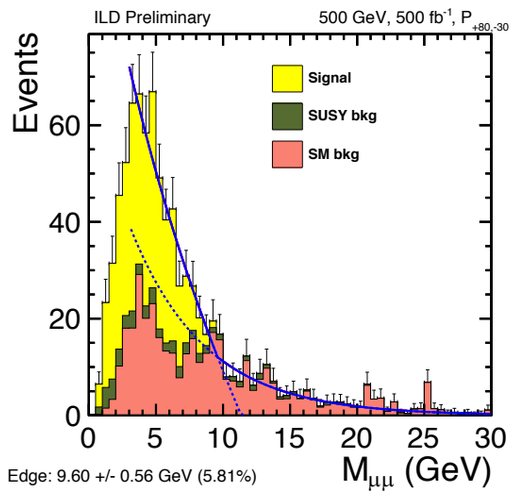 Edge: 9.60 +/- 0.56 GeV (5.81%)
E	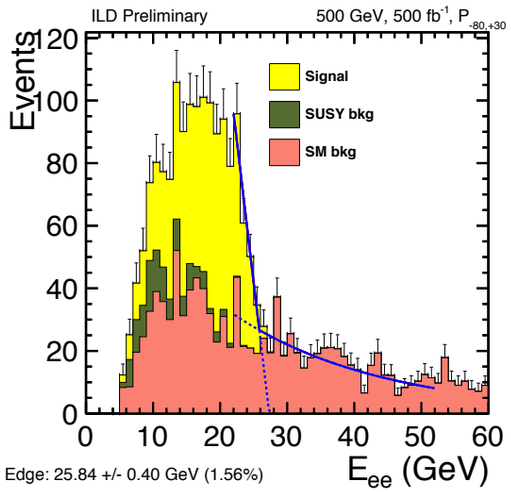 Edge: 25.84 +/- 0.40 GeV (1.56%)	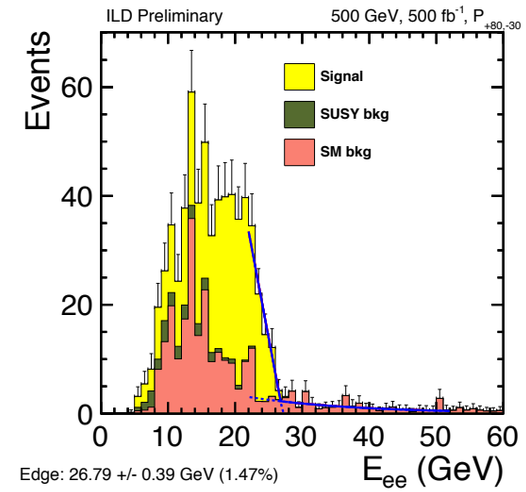 Edge: 26.79 +/- 0.39 GeV (1.47%)	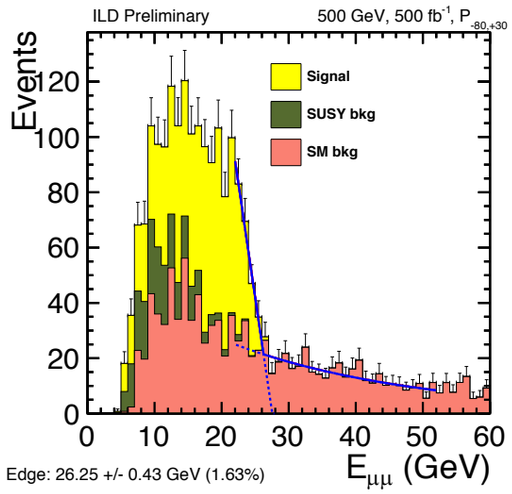 Edge: 26.25 +/- 0.43 GeV (1.63%)	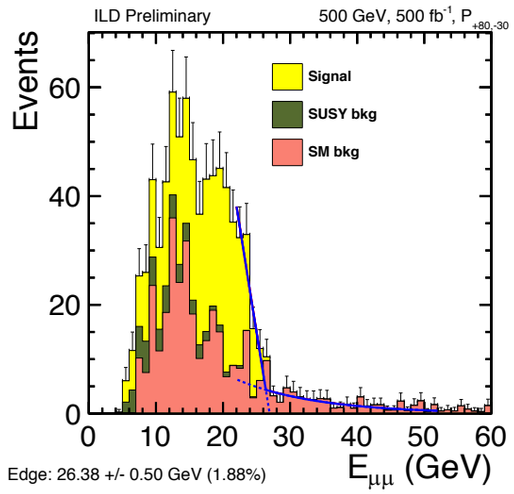 Edge: 26.38 +/- 0.50 GeV (1.88%)

The kinematic edge is modeled as: straight line (signal) + exponential (background). The precision is estimated using toy MC experiments.

Kinematic Edges: nGMM1 (N1N2)

ee, (-80,+30) | **ee, (+80,-30)** | **μμ, (-80,+30)** | **μμ, (+80,-30)**

M(J/ψ)

J/ψ masses are a bit off: will be investigated

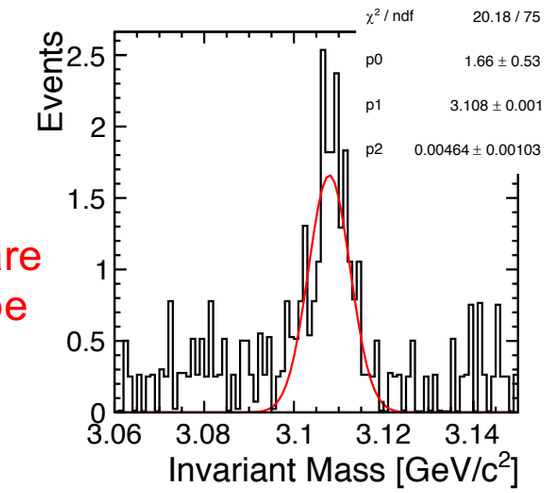

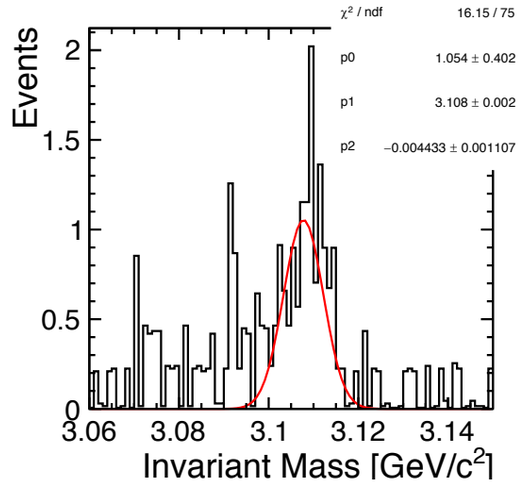

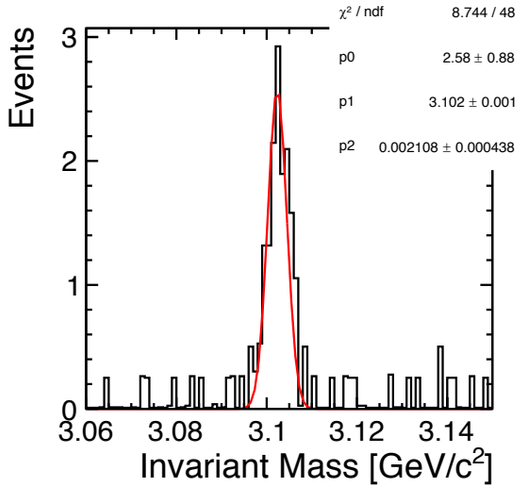

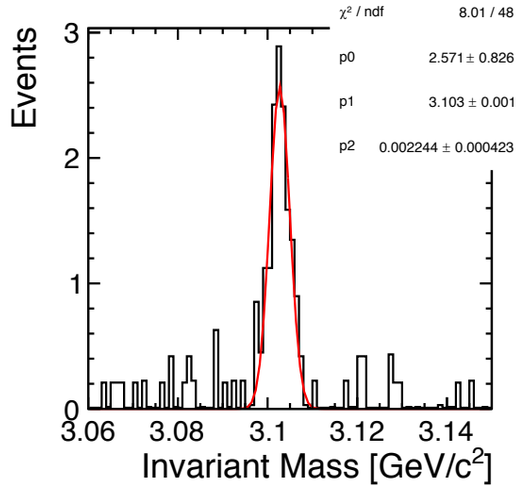

M

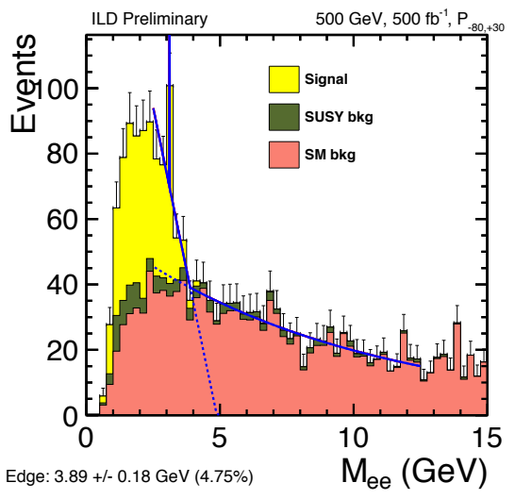

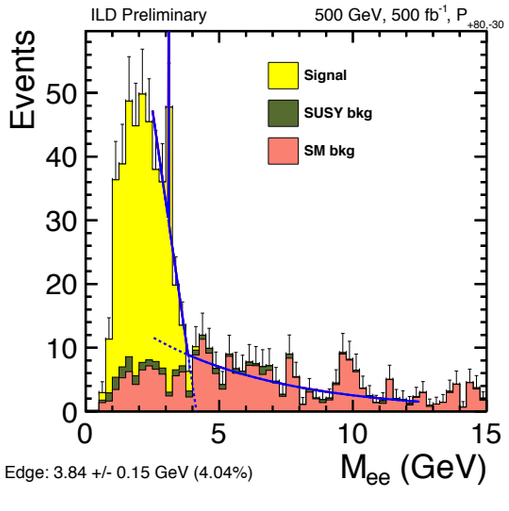

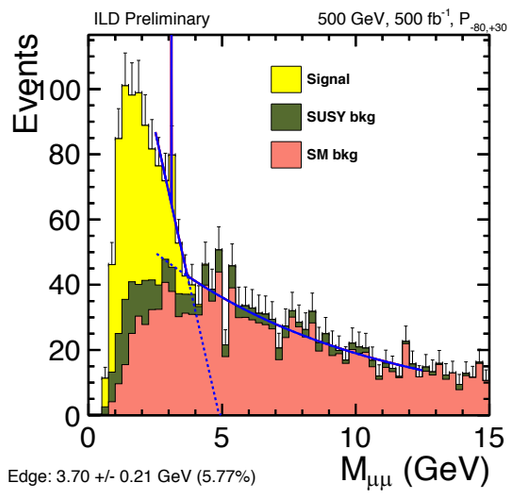

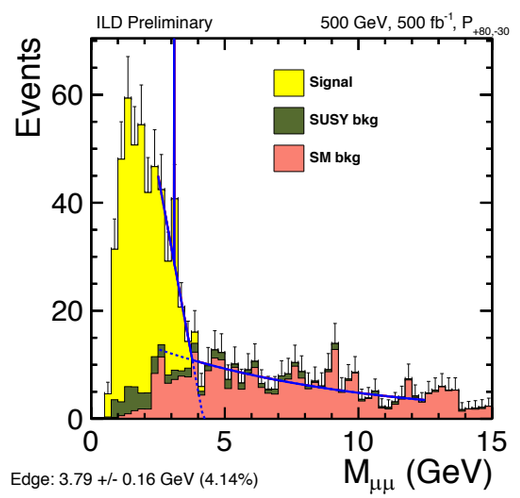

E

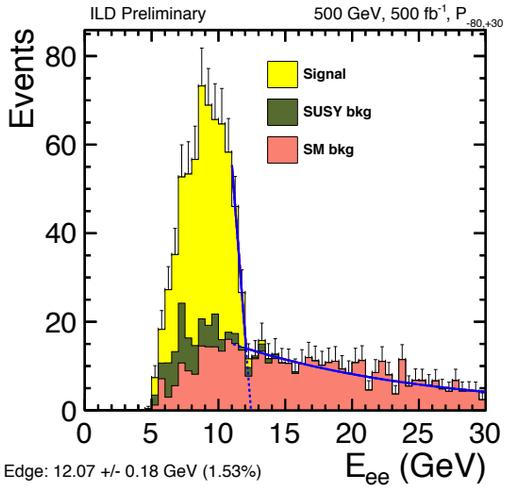

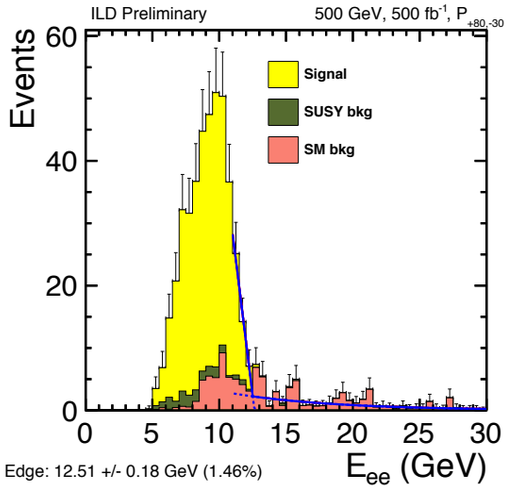

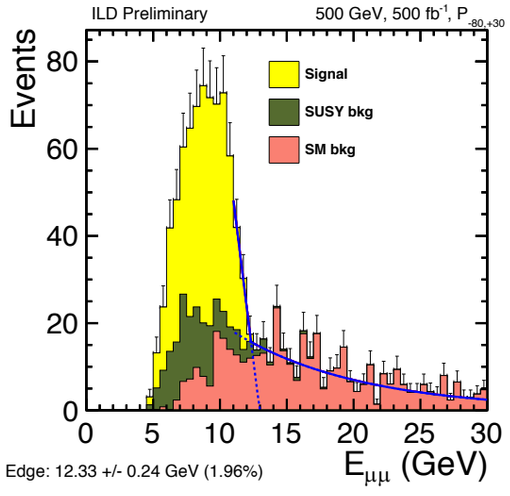

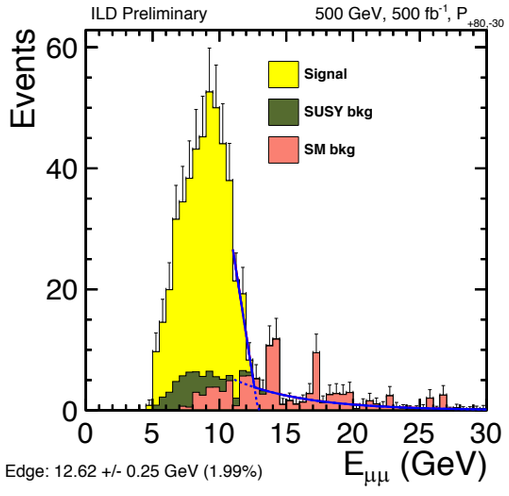

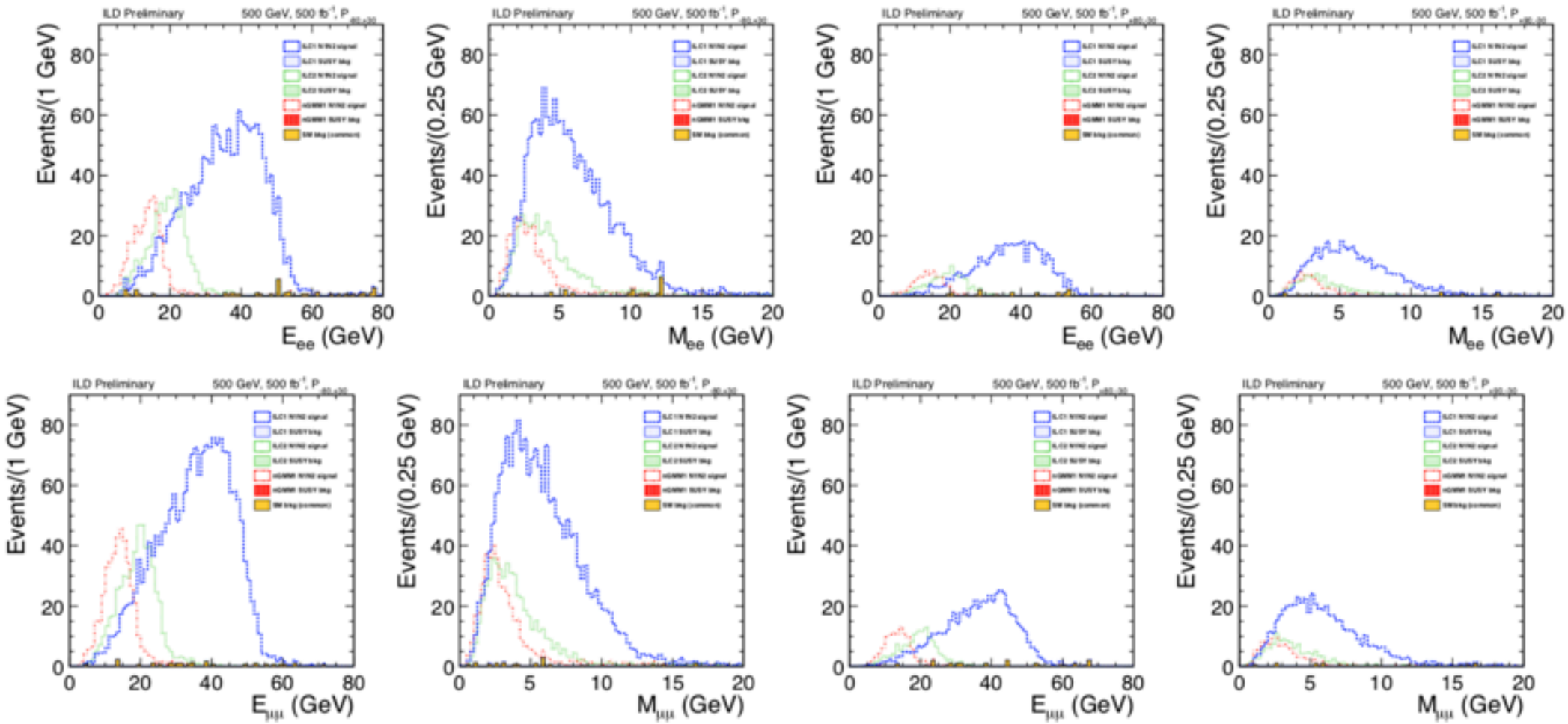

Figure 4: Chargino measurement

Di-jet Reconstruction

- Naïve reconstruction of di-jet mass suffers from heavy tail
- Dominant effect: neutral reconstruction **(NOT detector resolution)**
- Set only the neutral component of the jet to have zero mass → improves core reconstruction but the tail remains
- Set jet mass to zero → overcompensation in the core but reproduces the edge → used in this study.

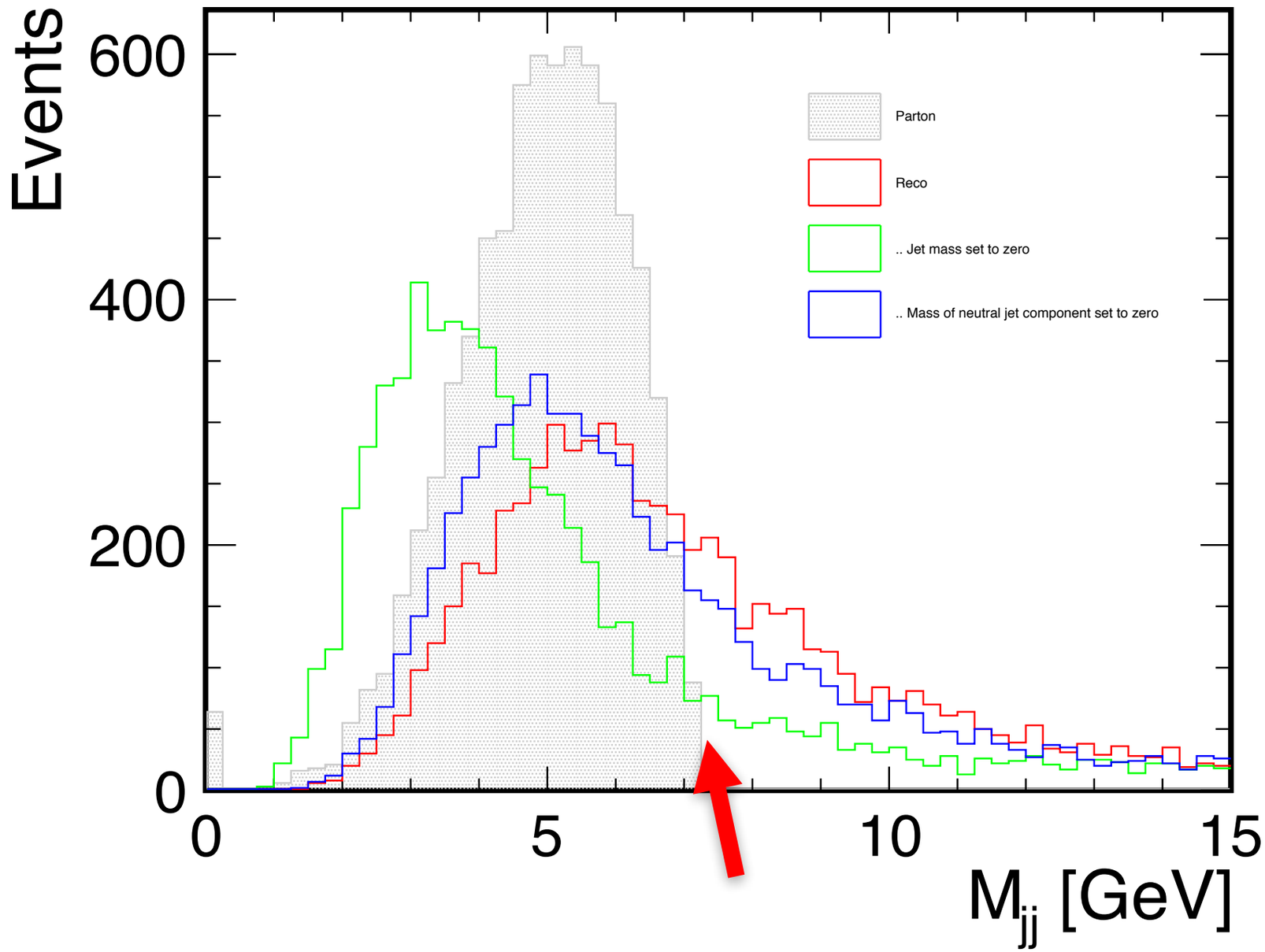

Kinematic Edges: ILC1 (C1C1)

	l=e, (-80,+30)	l=e, (+80,-30)	l=μ, (-80,+30)	l=μ, (+80,-30)
M	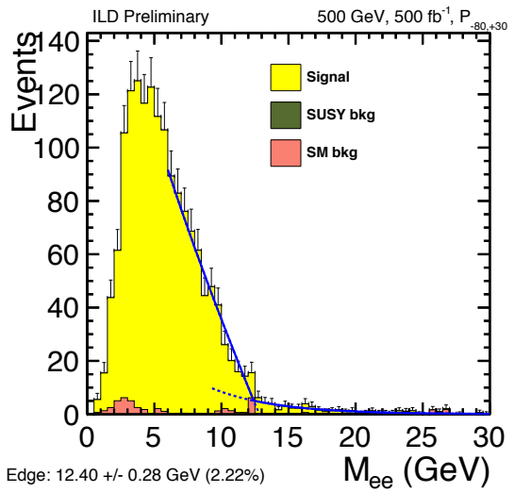	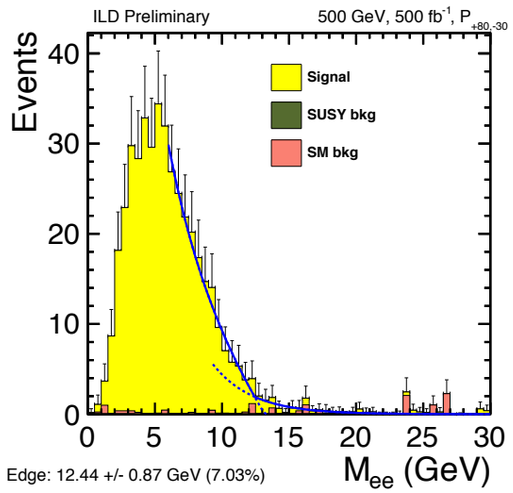	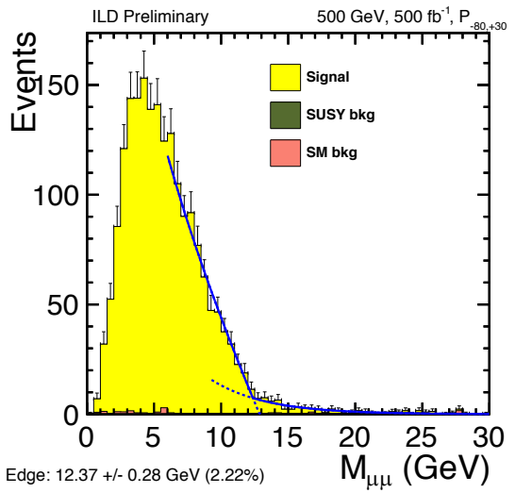	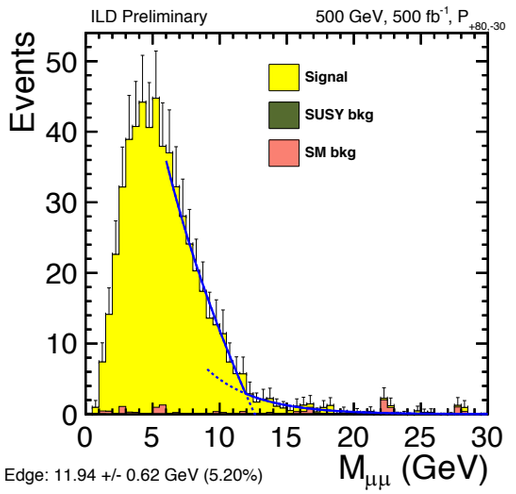
E	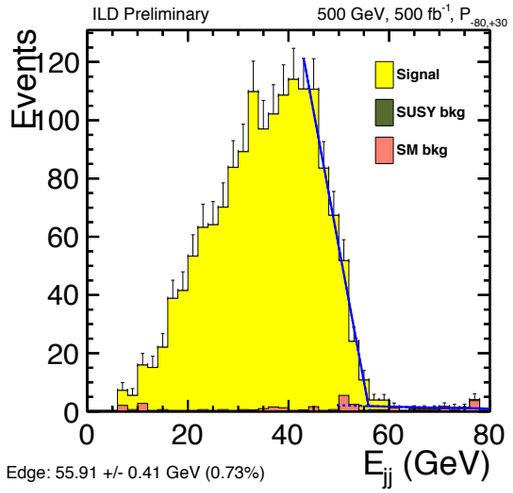	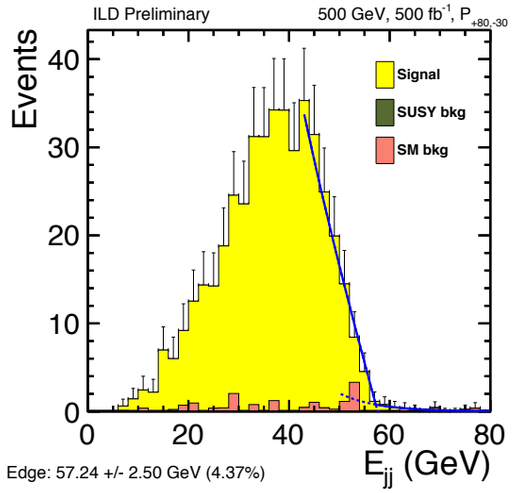	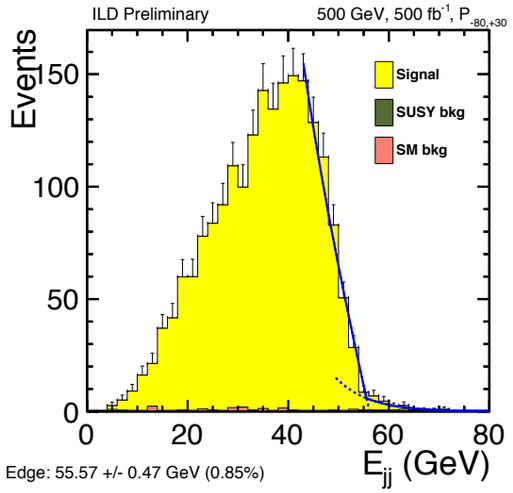	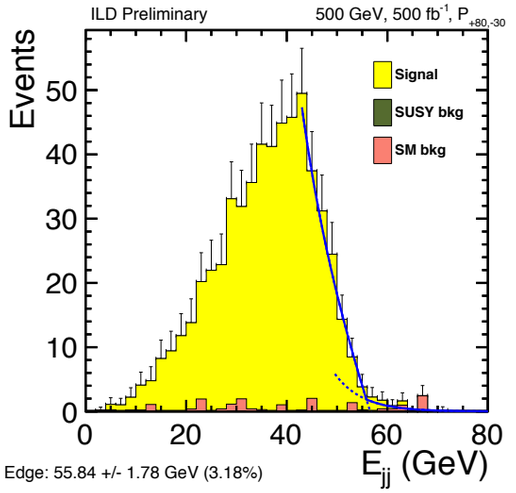

- The core is model with a straight line, while the tail is model with an exponential. The intersection is extract as the edge. The precision is estimated using toy MC experiments.
- A shift in the extract value (bias) is seen. This is correct by a scaling factor.

Kinematic Edges: ILC2 (C1C1)

	l=e, (-80,+30)	l=e, (+80,-30)	l=μ, (-80,+30)	l=μ, (+80,-30)
M	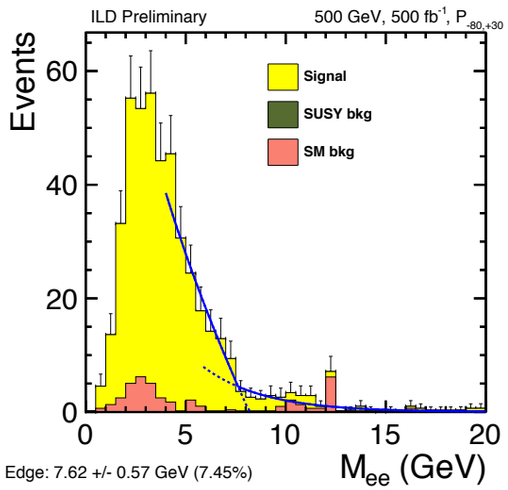	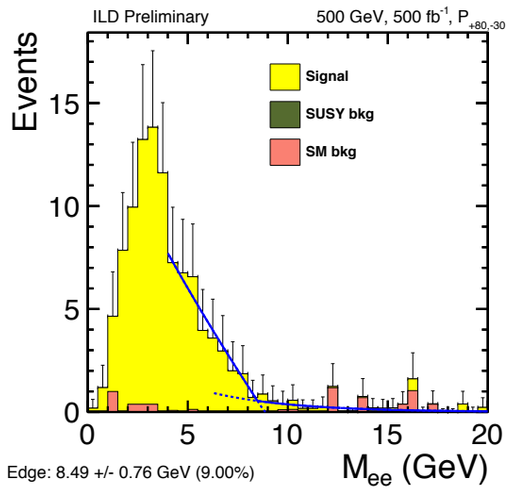	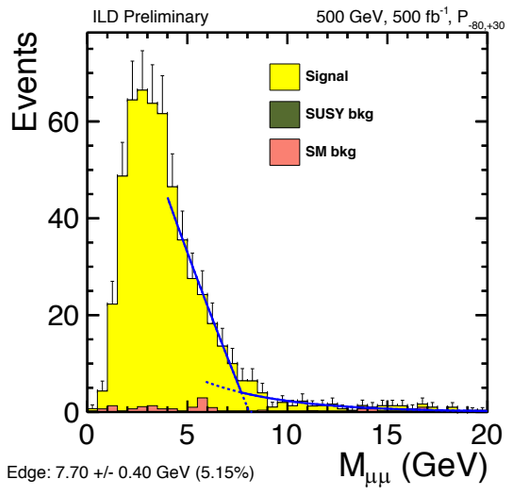	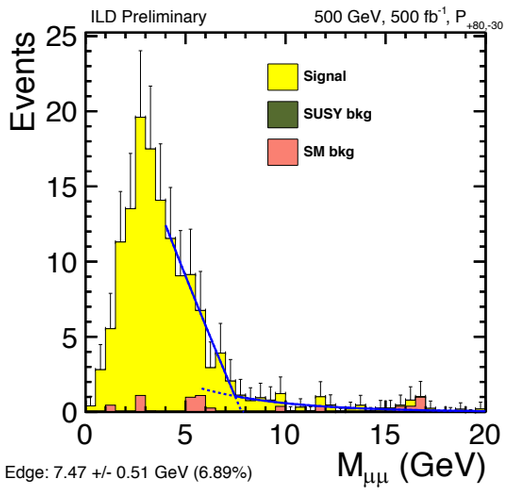
E	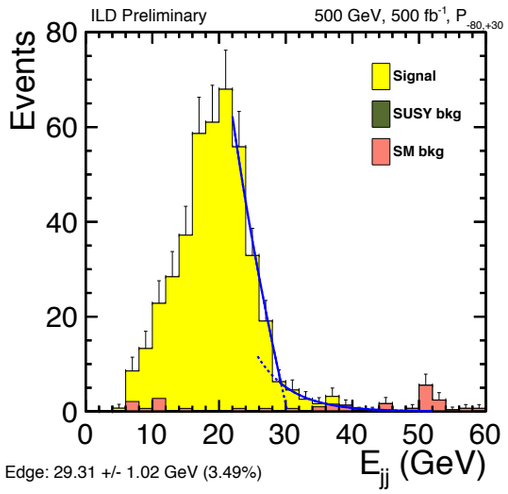	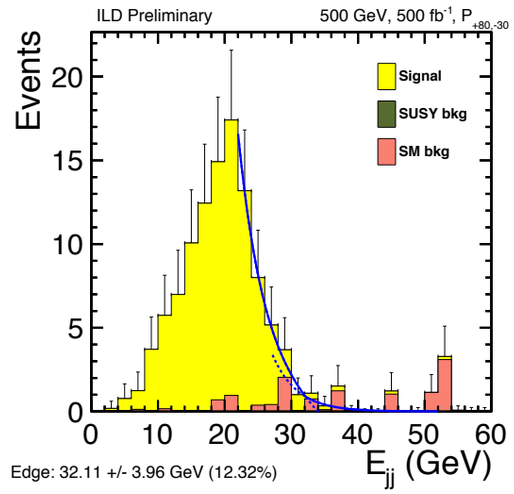	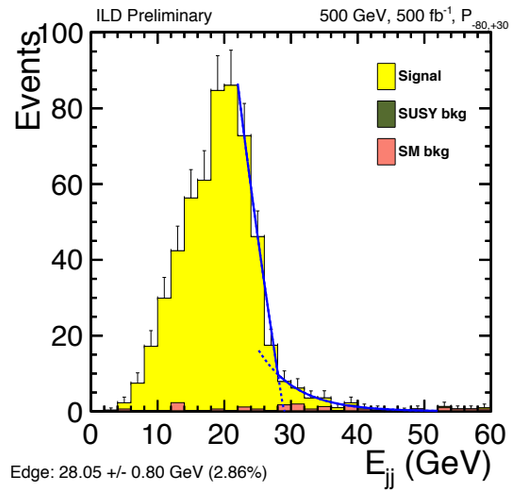	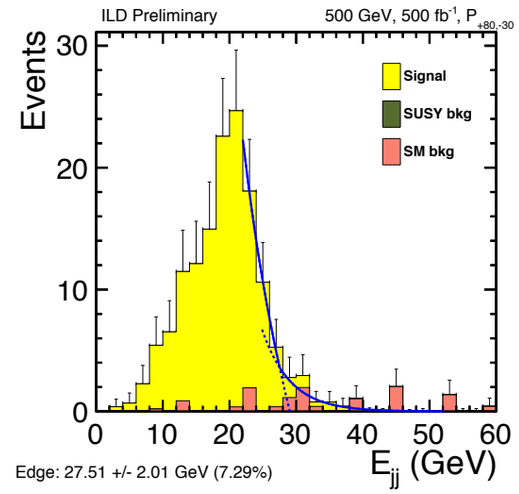

- The core is model with a straight line, while the tail is model with an exponential. The intersection is extract as the edge. The precision is estimated using toy MC experiments.
- A shift in the extract value (bias) is seen. This is correct by a scaling factor.

Kinematic Edges: nGMM1 (C1C1)

	l=e, (-80,+30)	l=e, (+80,-30)	l=μ, (-80,+30)	l=μ, (+80,-30)
M	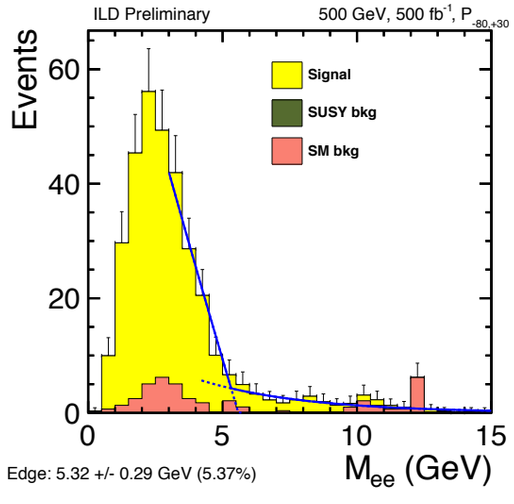	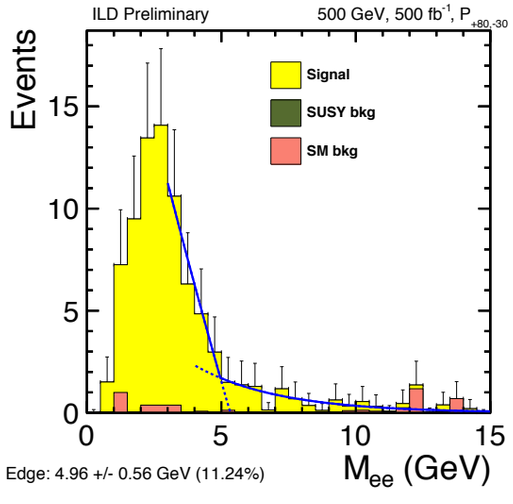	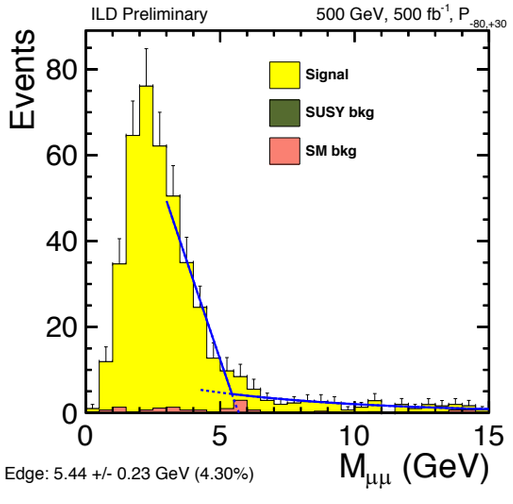	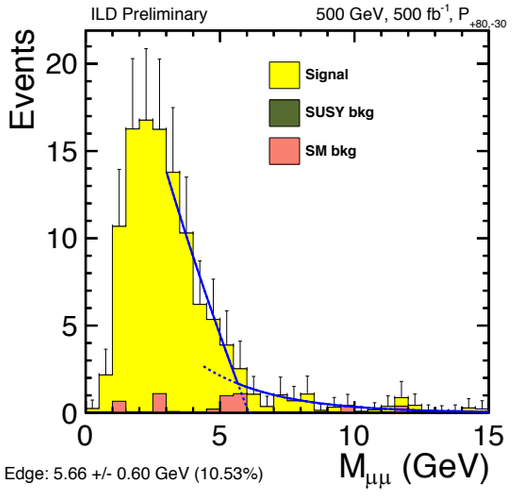
E	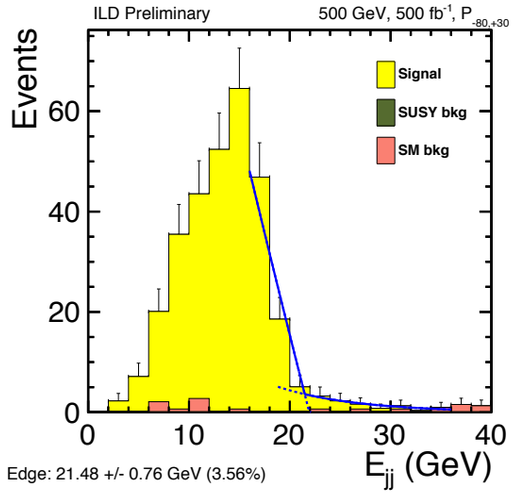	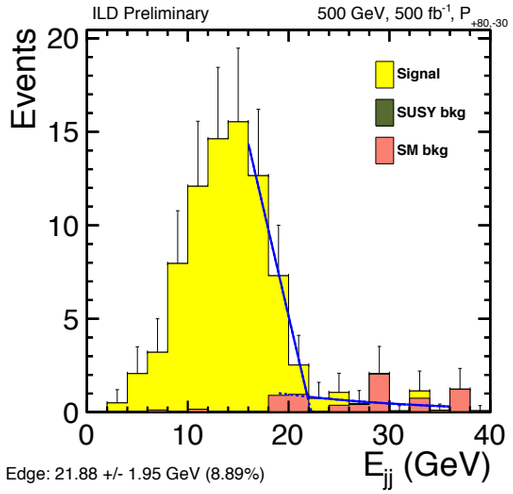	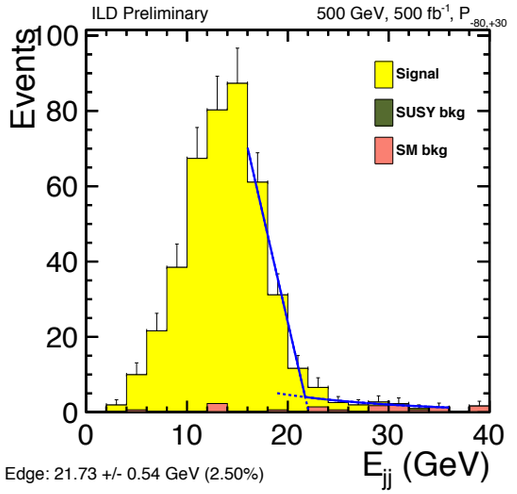	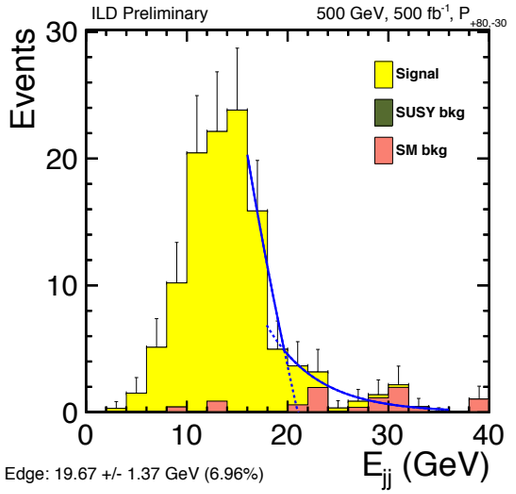

- The core is model with a straight line, while the tail is model with an exponential. The intersection is extract as the edge. The precision is estimated using toy MC experiments.
- A shift in the extract value (bias) is seen. This is correct by a scaling factor.

ILC1	model mass [GeV]	precision	H20 precision
$m_{\widetilde{\chi}_1^0}$	104.8	0.828%	0.463%
$m_{\widetilde{\chi}_2^0}$	127.5	0.800%	0.447%
$m_{\widetilde{\chi}_1^\pm}$	116.0	0.811%	0.453%
ILC2	model mass [GeV]	precision	I20 precision
$m_{\widetilde{\chi}_1^0}$	151.3	1.282%	0.717%
$m_{\widetilde{\chi}_2^0}$	162.4	1.330%	0.743%
$m_{\widetilde{\chi}_1^\pm}$	157.0	1.325%	0.741%
nGMM1	model mass [GeV]	precision	I20 precision
$m_{\widetilde{\chi}_1^0}$	154.9	1.722%	0.963%
$m_{\widetilde{\chi}_2^0}$	160.2	1.739%	0.972%
$m_{\widetilde{\chi}_1^\pm}$	157.4	1.705%	0.953%

Table 4: ILC1, ILC2 and nGMM1 MSSM model masses from `SPheno3.3.9beta`. Experimental mass precision combined from 500 GeV 500^{-1} fb for both $\mathcal{P}(\pm 0.8, \mp 0.3)$. It is assumed that the same precision is valid for these masses and mass differences as the simulation shows for the `Isajet` masses. Last column: precision scaled to 1600 fb^{-1} for both polarisations at $\sqrt{s} = 500$ GeV, ignoring the data sets with other centre-of-mass energies in H20 and I20 operating scenarios.

ILC1 $\Delta(\sigma \times BR)[\%]$	$\sqrt{s} = 500$ GeV $\mathcal{L} = 500$ fb^{-1}	$\sqrt{s} = 500$ GeV $\mathcal{L} = 1600$ fb^{-1}	$\sqrt{s} = 250$ GeV $\mathcal{L} = 1350$ fb^{-1}	$\sqrt{s} = 350$ GeV $\mathcal{L} = 135$ fb^{-1}
$LR\ \sigma(\widetilde{\chi}_2^0\widetilde{\chi}_1^0 \to \widetilde{\chi}_1^0\widetilde{\chi}_1^0 ee)$	3.80	2.12	1.65	5.36
$LR\ \sigma(\widetilde{\chi}_2^0\widetilde{\chi}_1^0 \to \widetilde{\chi}_1^0\widetilde{\chi}_1^0 \mu\mu)$	3.42	1.91	1.48	4.82
$LR\ \sigma(\widetilde{\chi}_1^+\widetilde{\chi}_1^- \to \widetilde{\chi}_1^0\widetilde{\chi}_1^0 qqe\nu_e)$	2.59	1.45	1.20	3.74
$LR\ \sigma(\widetilde{\chi}_1^+\widetilde{\chi}_1^- \to \widetilde{\chi}_1^0\widetilde{\chi}_1^0 qq\mu\nu_\mu)$	2.27	1.27	1.05	3.28
$\Delta(\sigma \times BR)[\%]$	$\mathcal{L} = 500$ fb^{-1}	$\mathcal{L} = 1600$ fb^{-1}	$\mathcal{L} = 450$ fb^{-1}	$\mathcal{L} = 45$ fb^{-1}
$RL\ \sigma(\widetilde{\chi}_2^0\widetilde{\chi}_1^0 \to \widetilde{\chi}_1^0\widetilde{\chi}_1^0 ee)$	3.38	1.89	2.56	8.29
$RL\ \sigma(\widetilde{\chi}_2^0\widetilde{\chi}_1^0 \to \widetilde{\chi}_1^0\widetilde{\chi}_1^0 \mu\mu)$	3.33	1.86	2.52	8.17
$RL\ \sigma(\widetilde{\chi}_1^+\widetilde{\chi}_1^- \to \widetilde{\chi}_1^0\widetilde{\chi}_1^0 qqe\nu_e)$	4.94	2.76	4.28	12.70
$RL\ \sigma(\widetilde{\chi}_1^+\widetilde{\chi}_1^- \to \widetilde{\chi}_1^0\widetilde{\chi}_1^0 qq\mu\nu_\mu)$	4.30	2.40	3.73	11.05

Table 5: ILC1: Simulation results for experimental precisions. Scaled precisions for the various centre of mass energies and the two polarisations. LR refers to the beam polarisation $\mathcal{P} = (-80\%, +30\%)$ and RL refers to $\mathcal{P} = (+80\%, -30\%)$.

ILC2 $\Delta(\sigma \times BR)[\%]$	$\sqrt{s} = 500$ GeV $\mathcal{L} = 500$ fb^{-1}	$\sqrt{s} = 500$ GeV $\mathcal{L} = 1600$ fb^{-1}	$\sqrt{s} = 250$ GeV $\mathcal{L} = 337.5$ fb^{-1}	$\sqrt{s} = 350$ GeV $\mathcal{L} = 1147.5$fb^{-1}
$LR\ \sigma(\widetilde{\chi}_2^0\widetilde{\chi}_1^0 \to \widetilde{\chi}_1^0\widetilde{\chi}_1^0 ee)$	5.52	3.09	–	3.30
$LR\ \sigma(\widetilde{\chi}_2^0\widetilde{\chi}_1^0 \to \widetilde{\chi}_1^0\widetilde{\chi}_1^0 \mu\mu)$	5.04	2.82	–	3.01
$LR\ \sigma(\widetilde{\chi}_1^+\widetilde{\chi}_1^- \to \widetilde{\chi}_1^0\widetilde{\chi}_1^0 qqe\nu_e)$	5.17	2.89	–	3.17
$LR\ \sigma(\widetilde{\chi}_1^+\widetilde{\chi}_1^- \to \widetilde{\chi}_1^0\widetilde{\chi}_1^0 qq\mu\nu_\mu)$	4.39	2.45	–	2.70
$\Delta(\sigma \times BR)[\%]$	$\mathcal{L} = 500$ fb^{-1}	$\mathcal{L} = 1600$ fb^{-1}	$\mathcal{L} = 112.5$ fb^{-1}	$\mathcal{L} = 382.5$ fb^{-1}
$RL\ \sigma(\widetilde{\chi}_2^0\widetilde{\chi}_1^0 \to \widetilde{\chi}_1^0\widetilde{\chi}_1^0 ee)$	6.54	3.66	–	3.93
$RL\ \sigma(\widetilde{\chi}_2^0\widetilde{\chi}_1^0 \to \widetilde{\chi}_1^0\widetilde{\chi}_1^0 \mu\mu)$	6.50	3.63	–	3.91
$RL\ \sigma(\widetilde{\chi}_1^+\widetilde{\chi}_1^- \to \widetilde{\chi}_1^0\widetilde{\chi}_1^0 qqe\nu_e)$	10.30	5.76	–	6.49
$RL\ \sigma(\widetilde{\chi}_1^+\widetilde{\chi}_1^- \to \widetilde{\chi}_1^0\widetilde{\chi}_1^0 qq\mu\nu_\mu)$	8.84	4.94	–	5.57

Table 6: ILC2: Simulation results for experimental precisions. Scaled precisions for the various centre of mass energies and the two polarisations. LR refers to the beam polarisation $\mathcal{P} = (-80\%, +30\%)$ and RL refers to $\mathcal{P} = (+80\%, -30\%)$.

nGMM1 $\Delta(\sigma \times BR)[\%]$	$\sqrt{s} = 500$ GeV $\mathcal{L} = 500$ fb^{-1}	$\sqrt{s} = 500$ GeV $\mathcal{L} = 1600$ fb^{-1}	$\sqrt{s} = 250$ GeV $\mathcal{L} = 337.5$ fb^{-1}	$\sqrt{s} = 350$ GeV $\mathcal{L} = 1147.5$ fb^{-1}
$LR\ \sigma(\widetilde{\chi}_2^0\widetilde{\chi}_1^0 \to \widetilde{\chi}_1^0\widetilde{\chi}_1^0 ee)$	6.81	3.81	–	4.11
$LR\ \sigma(\widetilde{\chi}_2^0\widetilde{\chi}_1^0 \to \widetilde{\chi}_1^0\widetilde{\chi}_1^0 \mu\mu)$	6.21	3.47	–	3.74
$LR\ \sigma(\widetilde{\chi}_1^+\widetilde{\chi}_1^- \to \widetilde{\chi}_1^0\widetilde{\chi}_1^0 qqe\nu_e)$	6.20	3.47	–	3.83
$LR\ \sigma(\widetilde{\chi}_1^+\widetilde{\chi}_1^- \to \widetilde{\chi}_1^0\widetilde{\chi}_1^0 qq\mu\nu_\mu)$	4.99	2.79	–	3.08
$\Delta(\sigma \times BR)[\%]$	$\mathcal{L} = 500$ fb^{-1}	$\mathcal{L} = 1600$ fb^{-1}	$\mathcal{L} = 112.5$ fb^{-1}	$\mathcal{L} = 382.5$ fb^{-1}
$RL\ \sigma(\widetilde{\chi}_2^0\widetilde{\chi}_1^0 \to \widetilde{\chi}_1^0\widetilde{\chi}_1^0 ee)$	5.88	3.29	–	3.56
$RL\ \sigma(\widetilde{\chi}_2^0\widetilde{\chi}_1^0 \to \widetilde{\chi}_1^0\widetilde{\chi}_1^0 \mu\mu)$	5.55	3.10	–	3.36
$RL\ \sigma(\widetilde{\chi}_1^+\widetilde{\chi}_1^- \to \widetilde{\chi}_1^0\widetilde{\chi}_1^0 qqe\nu_e)$	11.70	6.54	–	7.41
$RL\ \sigma(\widetilde{\chi}_1^+\widetilde{\chi}_1^- \to \widetilde{\chi}_1^0\widetilde{\chi}_1^0 qq\mu\nu_\mu)$	9.90	5.53	–	6.27

Table 7: nGMM1: Simulation results on experimental precisions. Scaled precisions for the various centre of mass energies and the two polarisations. LR refers to the beam polarisation $\mathcal{P} = (-80\%, +30\%)$ and RL refers to $\mathcal{P} = (+80\%, -30\%)$.

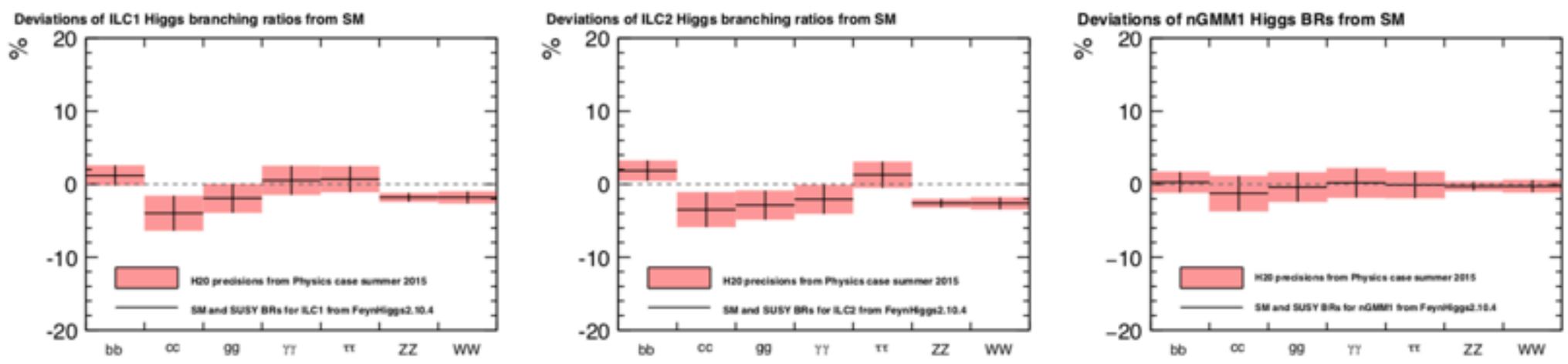

Figure 6: Deviations of the branching fractions of the SUSY light Higgs from the Standard Model expectations in ILC1, ILC2 and nGMM1.

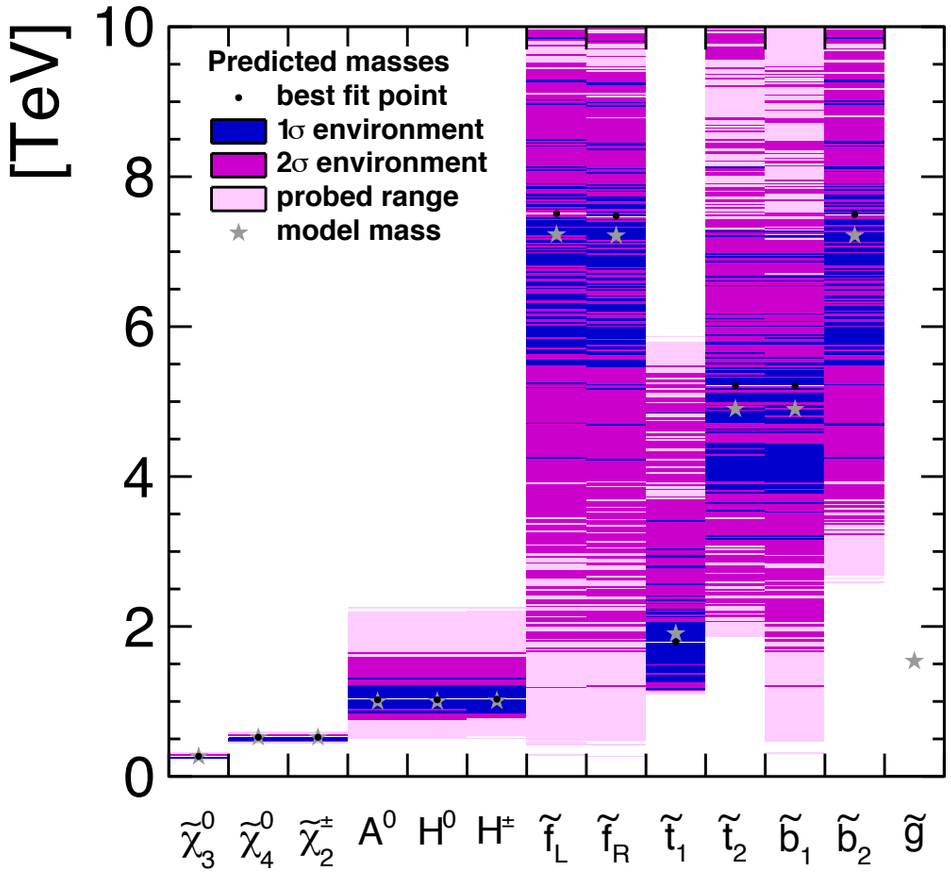
[TeV]
10
8
6
4
2
0
Predicted masses
best fit point
1σ environment
2σ environment
probed range
model mass
$\tilde{\chi}_3^0$ $\tilde{\chi}_4^0$ $\tilde{\chi}_2^\pm$ A^0 H^0 $H^\pm$ $\tilde{f}_L$ $\tilde{f}_R$ $\tilde{t}_1$ $\tilde{t}_2$ $\tilde{b}_1$ $\tilde{b}_2$ $\tilde{g}$

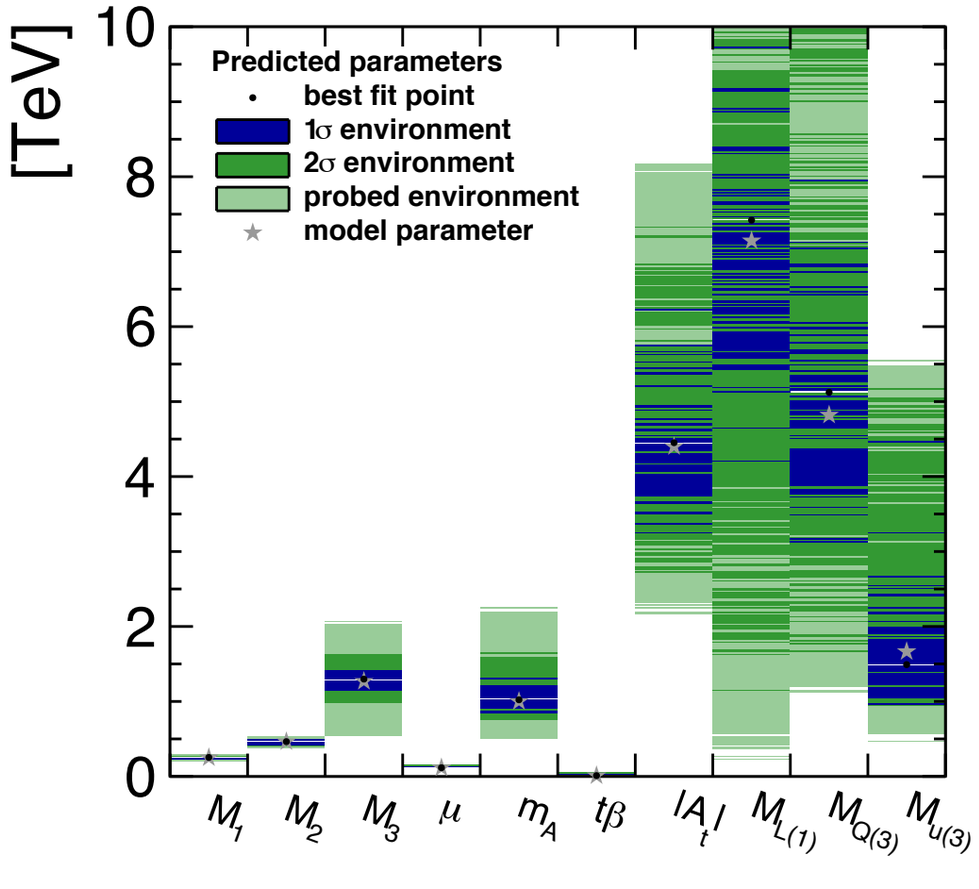
[TeV]
10
8
6
4
2
0
Predicted parameters
best fit point
1σ environment
2σ environment
probed environment
model parameter
M_1 M_2 M_3 μ m_A $t\beta$ $|A_t|$ $M_{L(1)}$ $M_{Q(3)}$ $M_{u(3)}$

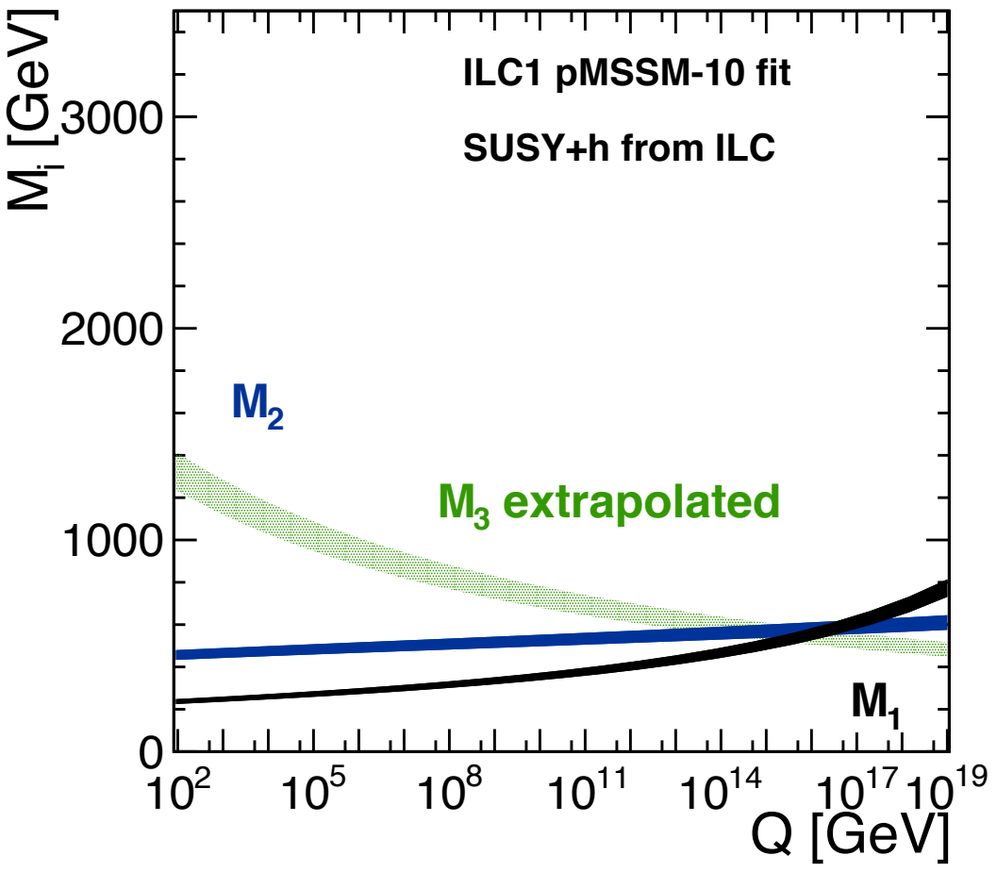
M_i [GeV]
3000
2000
1000
0
ILC1 pMSSM-10 fit
SUSY+h from ILC
M_2
M_3 extrapolated
M_1
10^2 10^5 10^8 10^{11} 10^{14} 10^{17} 10^{19}
Q [GeV]

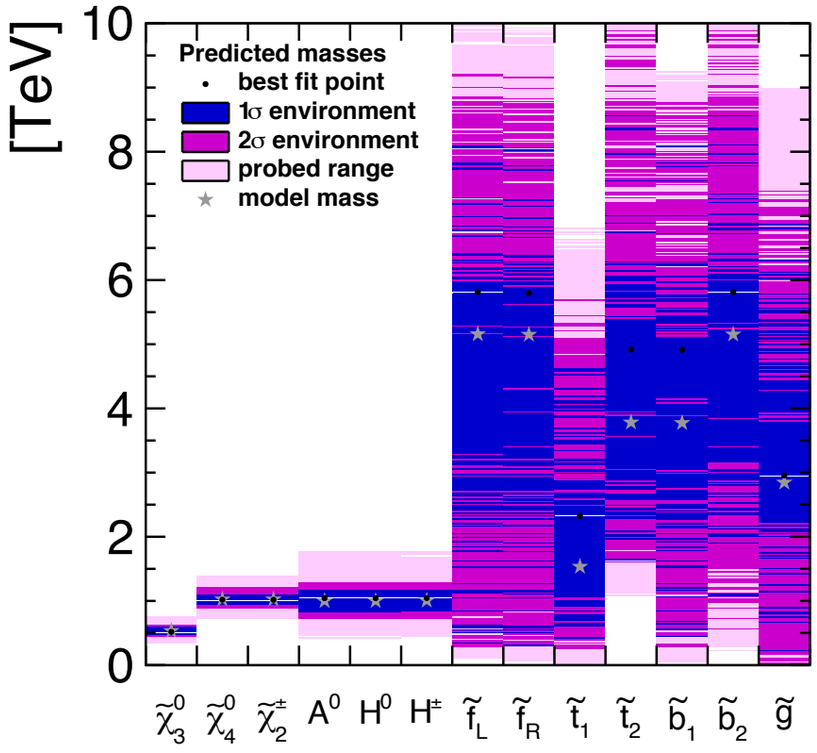
[TeV]
Predicted masses
best fit point
1σ environment
2σ environment
probed range
model mass
0
2
4
6
8
10
$\tilde{\chi}_3^0$ $\tilde{\chi}_4^0$ $\tilde{\chi}_2^\pm$ A^0 H^0 $H^\pm$ $\tilde{f}_L$ $\tilde{f}_R$ $\tilde{t}_1$ $\tilde{t}_2$ $\tilde{b}_1$ $\tilde{b}_2$ $\tilde{g}$

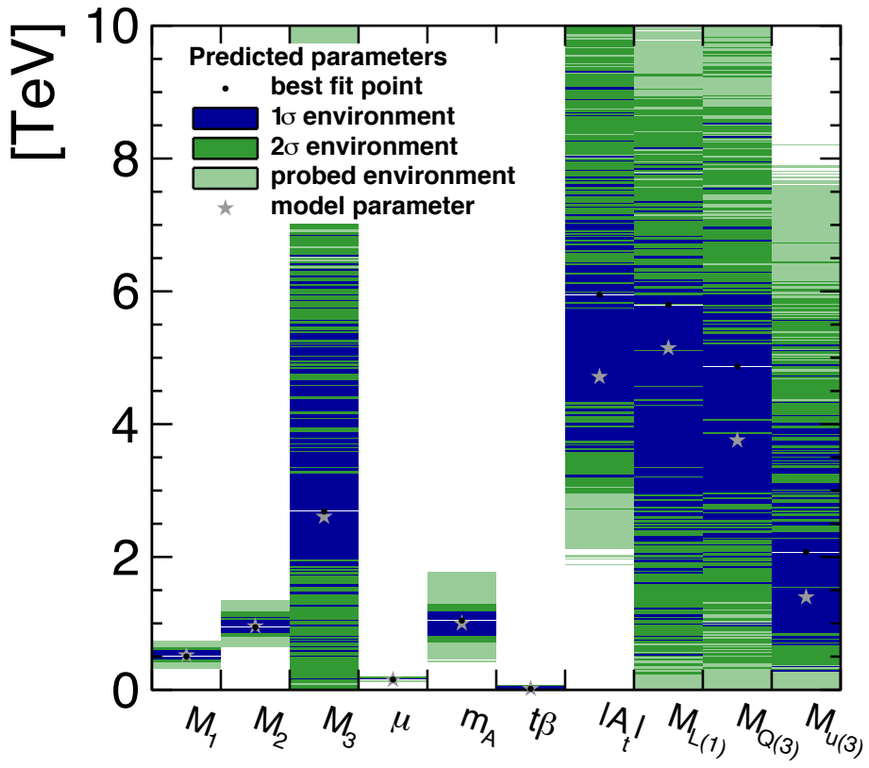
[TeV]
Predicted parameters
best fit point
1σ environment
2σ environment
probed environment
model parameter
0
2
4
6
8
10
M_1 M_2 M_3 μ m_A $t\beta$ $|A_t|$ $M_{L(1)}$ $M_{Q(3)}$ $M_{u(3)}$

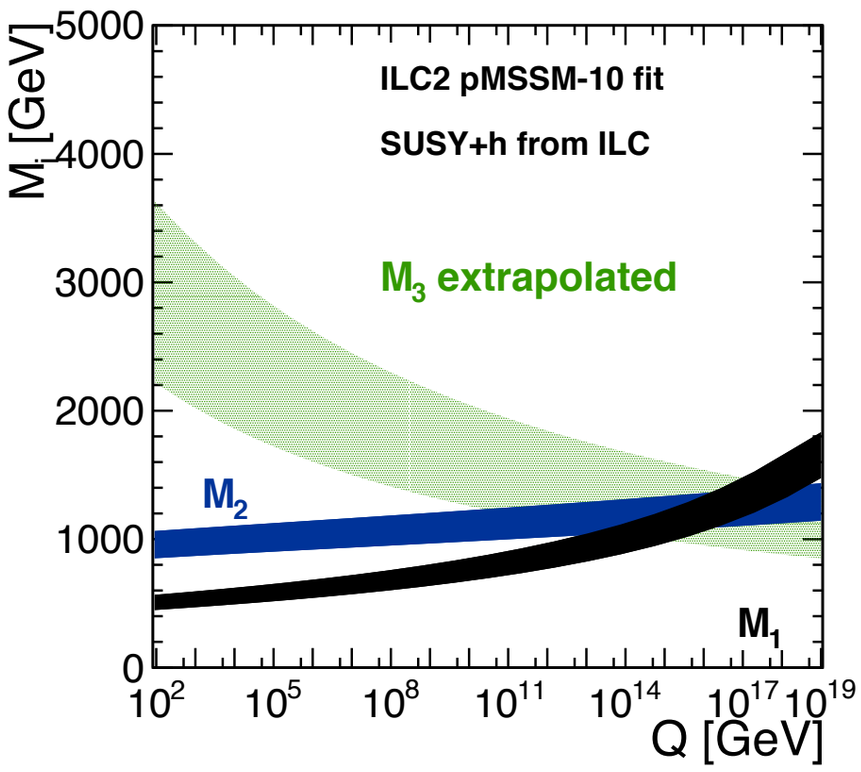
M_i [GeV]
ILC2 pMSSM-10 fit
SUSY+h from ILC
M_3 extrapolated
M_2
M_1
0
1000
2000
3000
4000
5000
10^2 10^5 10^8 10^{11} 10^{14} 10^{17} 10^{19}
Q [GeV]

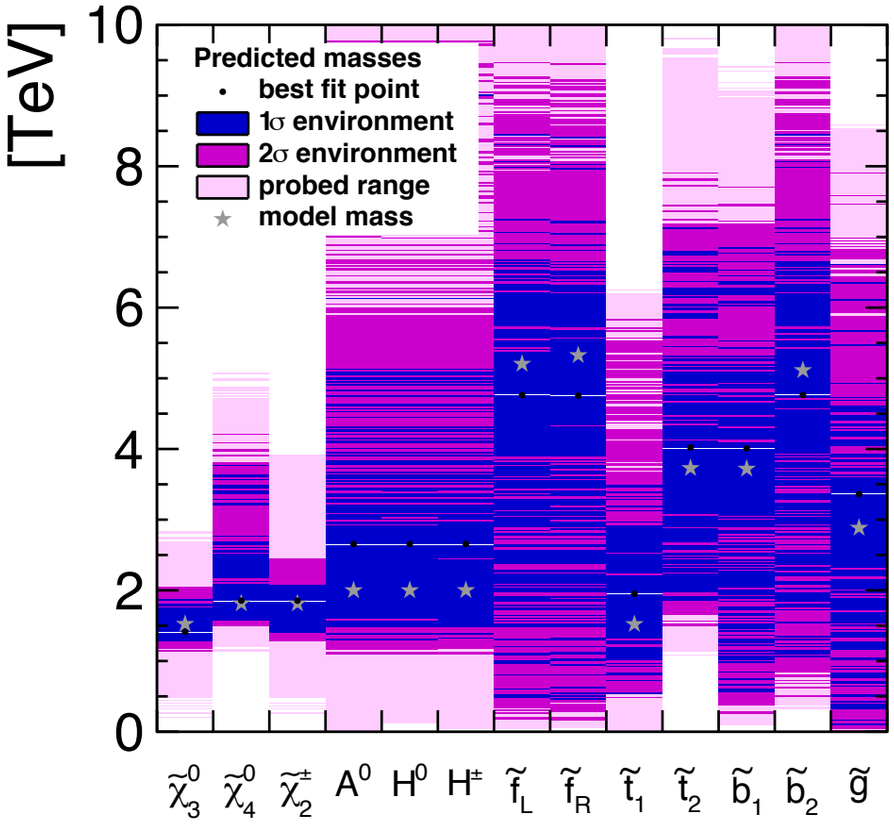
Predicted masses
best fit point
1σ environment
2σ environment
probed range
model mass
[TeV]
0
2
4
6
8
10
$\tilde{\chi}_3^0$ $\tilde{\chi}_4^0$ $\tilde{\chi}_2^\pm$ A^0 H^0 $H^\pm$ $\tilde{f}_L$ $\tilde{f}_R$ $\tilde{t}_1$ $\tilde{t}_2$ $\tilde{b}_1$ $\tilde{b}_2$ $\tilde{g}$

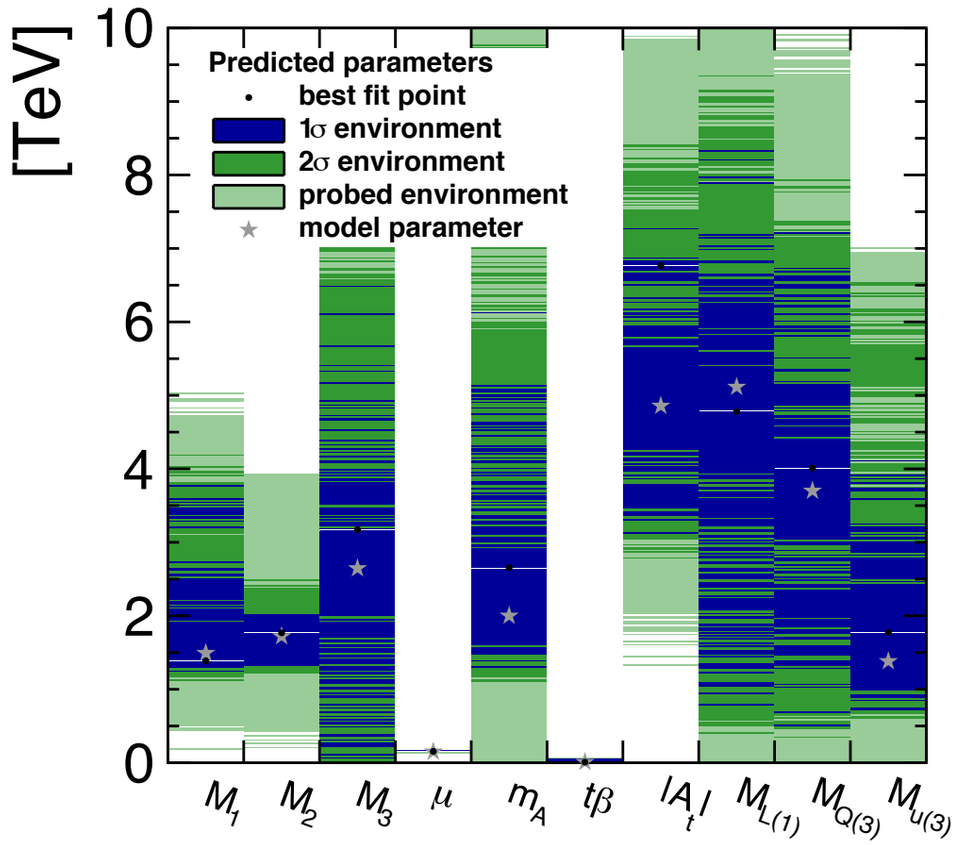
Predicted parameters
best fit point
1σ environment
2σ environment
probed environment
model parameter
[TeV]
0
2
4
6
8
10
M_1 M_2 M_3 μ m_A $t\beta$ $|A_t|$ $M_{L(1)}$ $M_{Q(3)}$ $M_{u(3)}$

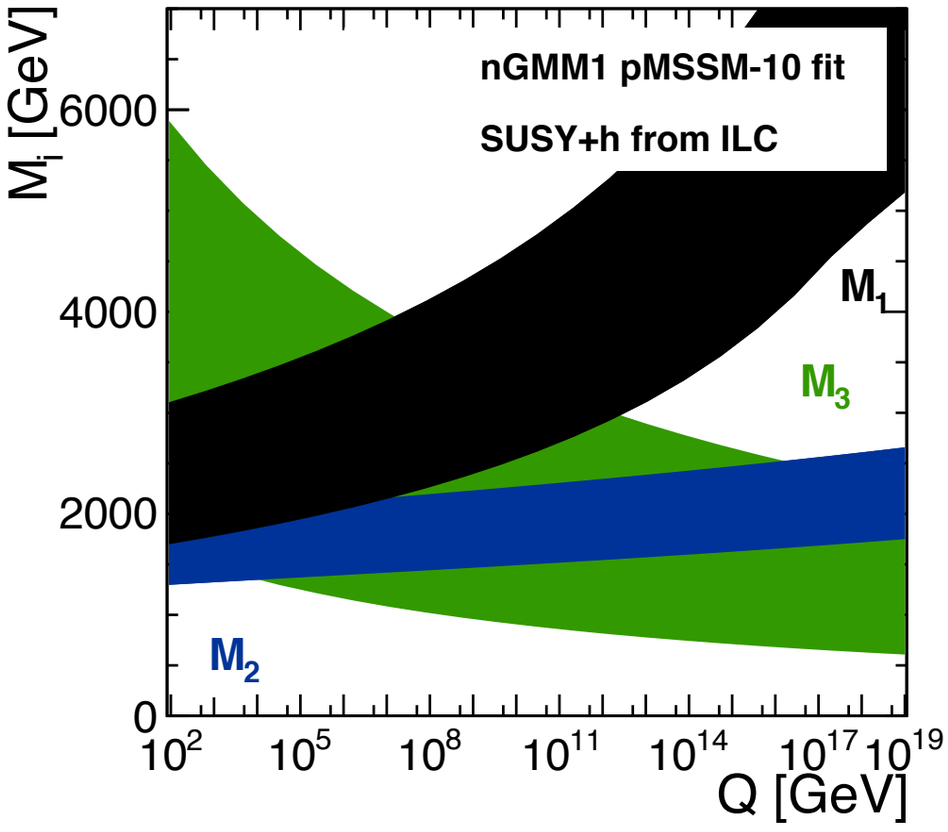
nGMM1 pMSSM-10 fit
SUSY+h from ILC
M_i [GeV]
0
2000
4000
6000
M_1
M_2
M_3
10^2 10^5 10^8 10^{11} 10^{14} 10^{17} 10^{19}
Q [GeV]